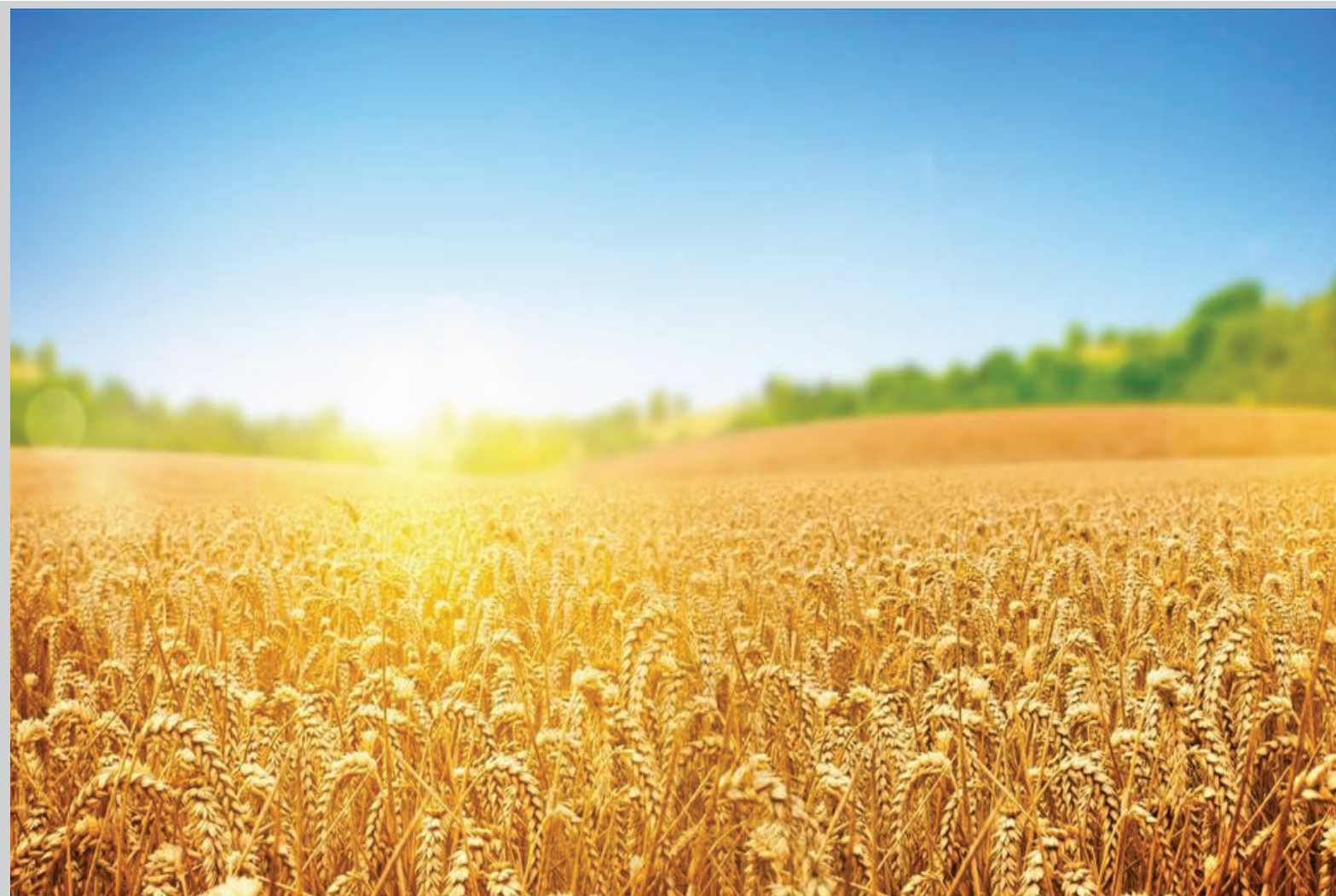


# Long-term evolution of the impacts of ozone air pollution on agricultural yields in Europe

A modelling analysis for the 1990-2010 period

November 2018



## Authors:

A. Colette, F. Tognet, L. Létinois, V. Lemaire, F. Couvidat, R.M. Alonso Del Amo,  
I. A. Gonzalez Fernandez, I. Rábago Juan-Aracil, H. Harmens, C. Andersson,  
S. Tsyro, A. Manders, M. Mircea

ETC/ACM consortium partners: National Institute for Public Health and the Environment (RIVM),  
Aether, Czech Hydrometeorological Institute (CHMI), Institut of Environmental Assessment and  
Water Research (CSIC/IDAEA), EMISIA, Institut National de l'Environnement Industriel et des  
Risques (INERIS), Norwegian Institute for Air Research (NILU), Öko-Institute, Öko-Recherche,  
Netherlands Environmental Assessment Agency (PBL), Universitat Autònoma de Barcelona  
(UAB), Umweltbundesamt Wien (UBA-V), Vlaamse Instelling voor Technologisch Onderzoek  
(VITO), 4sfera Innova

European Environment Agency  
European Topic Centre on Air Pollution and  
Climate Change Mitigation



Cover photo – © goodies.pcastuces.com

**Legal notice**

The contents of this publication do not necessarily reflect the official opinions of the European Commission or other institutions of the European Union. Neither the European Environment Agency, the European Topic Centre on Air Pollution and Climate Change Mitigation nor any person or company acting on behalf of the Agency or the Topic Centre is responsible for the use that may be made of the information contained in this report.

**Copyright notice**

© European Topic Centre on Air Pollution and Climate Change Mitigation (2018)  
Reproduction is authorized provided the source is acknowledged.

More information on the European Union is available on the Internet (<http://europa.eu>).

**Authors**

A. Colette, F. Tognet, L. Létinois, V. Lemaire, F. Couvidat: Institut National de l'Environnement Industriel et des Risques (INERIS, France)  
R. Alonso Del Amo, I. Gonzalez Fernandez, I. Rábago Juan-Aracil: Centro de Investigaciones Energéticas, Medioambientales y Tecnológicas (CIEMAT, Spain)  
H. Harmens: Centre For Ecology & Hydrology (CEH, United Kingdom)  
C. Andersson: Swedish Meteorological and Hydrological Institute Norrköping (SMHI, Sweden)  
A. Manders: Netherlands Institute for Applied Scientific Research (TNO, Netherlands)  
M. Mircea: National Agency for New Technologies, Energy and Sustainable Economic Development (ENEA, Italy)  
S. Tsyro: Norwegian Meteorological Institute, (Met Norway)

European Topic Centre on Air Pollution

and Climate Change Mitigation

PO Box 1

3720 BA Bilthoven

The Netherlands

Tel.: +31 30 274 8562

Fax: +31 30 274 4433

Web: <http://acm.eionet.europa.eu>

Email: [etcacm@rivm.nl](mailto:etcacm@rivm.nl)



## Contents

Acknowledgements .....	4
Abstract .....	5
1 Introduction.....	7
2 Methods .....	8
2.1 Ozone indicators.....	8
2.1.1 AOT40 .....	8
2.1.2 Phytotoxic Ozone Dose (POD <sub>y</sub> ) .....	9
2.1.3 Vertical downscaling.....	12
2.2 Inputs data.....	13
2.2.1 Crops.....	13
2.2.2 Observations.....	13
2.2.3 Modelling: Eurodelta-Trends multi model ensemble .....	14
3 Results .....	15
3.1 Model validation.....	15
3.2 Maps.....	18
3.2.1 AOT40 .....	18
3.2.2 POD <sub>6</sub> SPEC.....	20
3.3 Trends.....	22
3.3.1 Map of Trends .....	22
3.3.2 Trends of country-average AOT40 and POD <sub>6</sub> SPEC .....	24
3.3.3 Time series averaged over Europe for AOT40 and POD <sub>6</sub> SPEC .....	25
3.4 Loss .....	26
4 Conclusion/Discussion.....	30
References.....	32
Annex 1 – Ozone in Europe in the absence of anthropogenic emissions .....	34
Annex 2 – Exposure and losses by country .....	39

## Acknowledgements

- Modelling data used in the present analysis were produced in the framework of the EURODELTATrends Project initiated by the Task Force on Measurement and Modelling of the Convention on Long-range Transboundary Air Pollution. EURODELTATrends is coordinated by INERIS and involves modelling teams of BSC, CEREA, CIEMAT, ENEA, IASS, JRC, MET Norway, TNO, SMHI. The views expressed in this study are those of the authors and do not necessarily represent the views of EURODELTATrends modelling teams.

## Abstract

### Scope

- The aim of the present report is to assess long-term trends of potential detrimental impacts of ozone pollution for crop yields over Europe over the 1990-2010 period.
- Ozone impacts on vegetations are assessed using two metrics: the Accumulated Ozone over a Threshold concentration (AOT40 as defined in the European-Directive of 2008 on Ambient Air Quality), or the Phytotoxic Ozone Dose (POD) recommended by the Working Group on Effects of UNECE Convention on Long-range Transboundary Air Pollution. AOT40 is a concentration-based exposure metric, whereas POD represents the accumulated absorbed dose.

### Methods

- Both metrics are computed using ozone concentrations from either in situ observations (long-term EMEP monitoring data) and the Eurodelta-Trends ensemble of Chemistry Transport Models (CTMs) calculations.
- AOT40 can be readily computed from any ozone concentration time series. PODy calculations are more complex since they relate to the plant stomatal uptake which can be limited by environmental conditions such as temperature, light, relative humidity, soil moisture, and phenology. PODy can therefore be computed either within a Chemistry-Transport Model (online), or *a posteriori* (offline). We opted here for the offline approach, which requires to develop a standalone ozone deposition model. The main advantage of this approach is that it can be applied to an ensemble of available CTM simulations, or even in situ ozone observations. The main drawback is that it may be inconsistent with the deposition module of some CTMs.
- The focus is limited to wheat, for which we consider the POD<sub>6</sub>SPEC indicator as defined by the Working Group on Effects of UNECE Convention on Long-range Transboundary Air Pollution.

### Validation

- The performance of the CTMs in capturing ozone trends is tested. One model exhibits higher ozone concentrations than the other four models involved, but the consistency is better in terms of POD<sub>6</sub>SPEC, arguing in favor of the robustness of the POD calculation based on CTM results.
- The European maps of AOT40 exposure or POD<sub>6</sub>SPEC dose of the crop wheat are qualitatively similar in terms of spatial variability to estimates available in the literature.
- The performance of the models in capturing observed trends depends on the ozone metric. Overall the performances are better for the 2000-2010 than for the 1990-2000 decade because of a general overestimation of ozone exposure in the early 1990s, which leads to an overestimation of downward trends in the models. This overestimation has a larger impact on modelled AOT40 than POD<sub>6</sub>SPEC that appears better reproduced by the models. It should be noted that this validation is limited to Central and Northern Europe since no monitoring data are available in Southern Europe for the period 1990-2000.

### Results

- Whereas no change in modelled annual mean ozone concentrations was found, a significant decline in summertime peak ozone concentrations indicates that the ozone profile (lower peaks, higher background concentrations) has changed in Europe between 1990 and 2010.
- Crop exposure has decreased over Europe according to the AOT40 metric, whereas the trend is much more limited according to the POD<sub>6</sub>SPEC metric. This difference can be due (i) to different sensitivity to trends in ozone background and peaks for the two metrics, (ii) to the role of other environmental variable (such as soil moisture, temperature or water vapour) that bear upon the length of the growing season and stomatal uptake accounted for in the POD<sub>6</sub>SPEC dose. This raises concern about the choice of the metric to be used to assess ozone impacts on crops, but also for the future evolution of those impacts considering the lack of significant trends in POD<sub>6</sub>SPEC yield losses over the 1990-2010 period despite the implementation of ambitious air pollution mitigation measures in Europe.
- The average yield loss estimate over Europe is very similar to earlier studies based on the POD<sub>6</sub>SPEC indicator. For the year 2000 (when most other studies are available) we found an

overall impact of 13.9% loss in wheat production, against 13% and 14% found in two earlier studies.

- In terms of wheat yield losses, the AOT40 metric as modelled in the Eurodelta-Trends ensemble points toward an average statistically significant decrease over Europe from 18.2 to 10.2% between 1990 and 2010, whereas for the POD<sub>6</sub>SPEC metric losses declined much less with a non-significant change from 14.9 to 13.3% in 1990 and 2010, respectively.
- The comparison between models and measurement indicates that the downward trend of AOT40 is overestimated by the models, especially for the 1990-2000 decade. This comparison only holds for Germany, Austria, Benelux, and the United Kingdom because of the lack of long-term measurements in other parts of Europe. For the 2000-2010 decade, when the agreement between model and observations is better, a discrepancy between AOT40 (decrease from 13.5 to 10.2%) and POD<sub>6</sub>SPEC (no statistically significant trend between 13.9 and 13.3%) yield losses is still found.

## 1 Introduction

The adverse impacts of air pollution on human health and ecosystems are substantial. For the Europe Union, the latest assessment (EEA, 2018) points toward almost 391,000, 76,000 and 16,400 anticipated death each year attributed to exposure to fine particulate matter ( $PM_{2.5}$ ), nitrogen dioxide and ozone ( $O_3$ ), respectively, for the year 2015. The same reports also mention substantial impacts on ecosystems, in particular through atmospheric deposition of acidifying and eutrophying compounds: about 6% of European ecosystems are at risk regarding acidification, whereas this fraction reaches 72% for eutrophication.

The recent air quality report published by EEA (2018) also emphasizes the detrimental impacts of ozone on natural vegetation and agricultural crops. The European Directive on Ambient Air Quality (EC, 2008) relies on the AOT40 indicator to assess those impacts. AOT40 is defined as the Accumulated (hourly) Ozone concentration over the Threshold of 40 ppbv (or  $80 \mu\text{g}/\text{m}^3$ ) between 8.00-20.00 hours Central European Time (CET) over the May-June-July period. The target value of AOT40 ( $18\,000 \mu\text{g}/\text{m}^3$  hour averaged over five years) is exceeded in about 30% of European agricultural areas, and the long-term objective ( $6\,000 \mu\text{g}/\text{m}^3$  hour) is exceeded in 80% of such areas. It should be noted that the European Directive definition for AOT40 differs slightly from the definition applied by the Long-range Transboundary Air Pollution (LRTAP) Convention (CLRTAP, 2017) (see Section 3.1.1). The LRTAP Convention critical level for agricultural crops based on wheat is 3 ppm hour (or  $6\,000 \mu\text{g}/\text{m}^3$  hour).

Besides the assessment of fraction of agricultural areas exposed to ozone pollution levels exceeding the regulatory values, one may also wish to assess the impact on agricultural yields. To achieve this, two risk assessment methodologies are available to estimate impacts. There are some exposure response relationships available in the literature to assess the amount of yield lost for a given AOT40 exposure. These should however be considered with caution, the Working Group on Effects of the LRTAP Convention recommends not to use the AOT40 approach to assess crop yield and subsequent economic losses since ozone effects are more strongly related to the uptake of ozone by plants than to the atmospheric concentration. Instead, in their Modelling and Mapping Manual (CLRTAP, 2017), they advocate the use of the Phytotoxic Ozone Dose (POD). The POD metric is biologically more relevant as it estimates the ozone flux absorbed via the leaf pores (stomata) into the plant. Whereas AOT40 only depends on the atmospheric ozone concentration, POD also accounts for the effects of meteorology (temperature, incoming solar radiation, water vapour pressure deficit), soil moisture and plant development (phenology) on the ozone flux into the plant. The rationale to include a sensitivity to soil moisture is because high ozone episodes frequently occur in dry areas and/or during dry periods. In dry conditions, plants often close their stomata to reduce water loss, thereby incidentally reducing their uptake of atmospheric ozone. Ignoring that effect (for instance by relying exclusively on AOT40) leads to a substantial overestimation of ozone impacts on ecosystems, particularly in Mediterranean areas (Emberson et al., 2000b), and can lead to an underestimation of impacts in Northern and Central Europe. Hence, AOT40 and POD provide a different spatial distribution of the risk of ozone impacts on vegetation (Simpson et al., 2007). It should be noted that those approaches were developed on the basis of a critical level perspective, therefore ensuring no impact below the corresponding thresholds, so that the dose/exposure response relationships are available for the most sensitive crop species and cultivars. Computed yield loss estimates based on this precautionary principle could thus be over-estimating actual impacts. The dose/exposure-response relationships applied in the current study better reflect the effect of ozone on the most sensitive wheat cultivars grown in the 1990's. Over the 20 years period covered by this report, newer wheat cultivars with a wide range of ozone sensitivity have been released.

The present report compares both AOT40 and POD approaches. In order to offer a complete coverage over Europe and over a long enough period to assess trends, the Eurodelta-Trends (EDT) ensemble is used. Eurodelta-Trends is a multi-model inter-comparison exercise coordinated by the Task Force on Measurement and Modelling (TFMM) of the LRTAP Convention. The project involved several Chemistry-

Transport Models that used a consistent setup to simulate air quality in Europe over the 1990-2010 time period (Colette et al., 2017a).

The hourly-modelled ozone fields are converted to either AOT40 or POD using an offline approach using the methodology introduced in Section 3. The results presented in Section 4 include comparison with observations, mapping the impacts of ozone on crop yields and assessing their trends. The report is limited to wheat, although the methodology is in principle also relevant to other crops and vegetation (trees and (semi-)natural vegetation (CLRTAP, 2017)).

## 2 Methods

### 2.1 Ozone indicators

Two indicators (or metrics) are used in this report to assess the impact of ozone on wheat yield. The AOT40 is the metric defined in the 2008 European Directive on Ambient Air Quality (EC, 2008). The acronym stands for Accumulated Ozone exposure over a Threshold of 40 parts per billion ( $80 \mu\text{g}/\text{m}^3$ ) and details of the computation of the metric and related impacts on yield are provided in Section 3.1.1.

An alternative and biologically more relevant metric has been developed in recent decades, in particular through the work of the Working Group on Effects of the LTRAP Convention. The ozone flux-based metric is referred to as POD, which stands for phytotoxic ozone dose and provides an estimation of the flux of ozone into the plant above a given threshold. Details of the computation of that metric and related impacts on wheat yield are provided in Section 3.1.2. It should be noted that POD is the preferred indicator for assessing the risk of adverse effects of ozone on vegetation (including crops) and any subsequent economic assessments.

#### 2.1.1 AOT40

The AOT40 is calculated according to the methodology defined in the Directive 2008/50/CE. It is defined as the sum of the difference between hourly concentrations greater than  $80 \mu\text{g}/\text{m}^3$  (or 40 ppb) and  $80 \mu\text{g}/\text{m}^3$  over a given period using only the one-hour values measured between 8.00 and 20.00 CET each day. Since we focus here exclusively on crops and not forest, the accumulation period is from 1 May to 31 July each year. The unit is  $(\mu\text{g}/\text{m}^3)\cdot\text{hours}$ , although it can also alternatively be presented as ppb.hour or even ppm.hour provided a conversion from mass to volume ratio.

In order to estimate the impacts on crop yield of a given exposure to AOT40, the specific exposure-response function used here was obtained from (Mills et al., 2007) and illustrated in Figure 1. It should be noted that the AOT40 calculation according to the Directive 2008/50/CE is slightly different than the method applied by (CLRTAP, 2017). In particular, in the Directive AOT is accumulated over the 8:00 to 20:00 hours CET, whereas in the Convention the accumulation depends on daylight hours, i.e. when radiation exceeds  $50\text{W}/\text{m}^2$ , and concentrations are downscaled to canopy height. Also, the Convention defines the three months accumulation period depending on the climatic region instead of the fixed May-July period used in the Directive. In addition, the CLRTAP Modelling and Mapping Manual provides a warning about the uncertainties related to the AOT40 methodology, emphasizing that it should not be used to assess economical losses.

The actual exposure-response function provides an estimate of the relative (unitless) yield for wheat for a given AOT40 exposure level according to:

$$\text{Relative wheat yield} = 0.99 - 0.0161 \text{ AOT40}$$

Hence, the maximum wheat yield loss is calculated as:

$$(1 - \text{relative yield}) * \text{yield}$$

Or  $(0.01 + 0.0161 * \text{AOT40}) * \text{yield}$

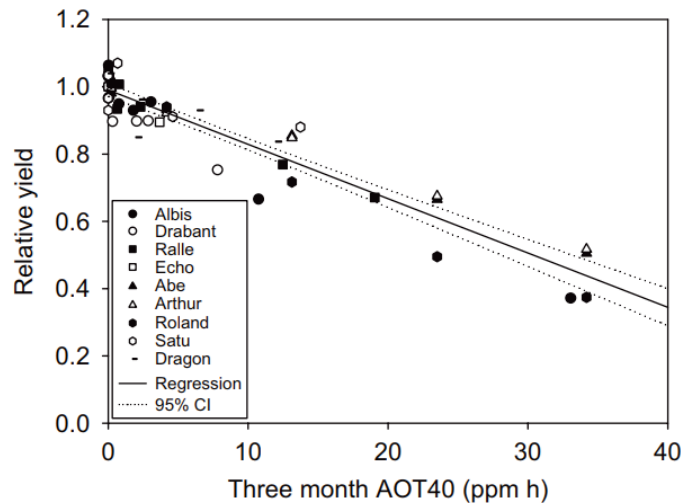


Figure 1: Exposure-response function for wheat yield (Note: dotted lines are 95% confidence limits), the individual symbols are for various types of cultivars source: (Mills et al., 2007).

### 2.1.2 Phytotoxic Ozone Dose (PODy)

The phytotoxic ozone dose (POD) (Emberson et al., 2000a; Emberson et al., 2000b) provides an estimate of the actual ozone flux entering the leaves (and therefore possibly damaging them), taking into account both environmental parameters (atmospheric ozone, soil moisture, temperature, light, vapour pressure deficit) and plant development (phenology).

A computer program to estimate phytotoxic ozone doses and the associated impact on wheat yield from a given atmospheric ozone concentration has been developed by INERIS. It follows precisely the methodology described in the Modelling and Mapping Manual (CLRTAP, 2017).

Note that unlike in existing implementations such as in the EMEP/MSC-W model (Simpson et al., 2012), we use here an offline POD module. Being offline, the module can be used to compute POD from any available ozone hourly time series (and additional meteorological variables) and for different potential vegetation types. The main benefit of the approach is that it applies to both observations and an ensemble of available modelled fields. There is also an important drawback. In online implementations of POD, the flux is used both to assess crop impacts and the atmospheric ozone sink, thereby ensuring consistency. In an offline implementation, the flux that goes into the plants assessed with POD is potentially inconsistent with the atmospheric sink in the CTM.

Several POD indicators and critical levels are described in the Modelling and Mapping Manual, including species-specific ones such as for wheat ( $\text{POD}_6\text{SPEC}$ ) and ones that are recommended for use in large-scale and integrated assessment modelling, for example  $\text{POD}_3\text{IAM}$  for crops.  $\text{POD}_3\text{IAM}$  is a simplified version of  $\text{POD}_6\text{SPEC}$  and does not include the modifying effect of soil moisture and plant development on ozone flux into the leaves. Here we use  $\text{POD}_6\text{SPEC}$  for wheat, which is calculated as the hourly averaged stomatal ozone flux above a threshold of  $6 \text{ nmol O}_3 \text{ m}^{-2} \text{ PLA (project leaf area)} \text{ s}^{-1}$  during daylight hours. Calculations of  $\text{POD}_6\text{SPEC}$  have been carried out using the parameterization for common bread wheat (*Triticum aestivum*) as it represents the most cultivated wheat species in Europe. The formulation of the Modelling and Mapping Manual (CLRTAP, 2017) for the biogeographical regions of Atlantic, Boreal, Continental, Pannonic and Steppic is applied for all the domain including the

Mediterranean region. The additional parameterization available for *Triticum aestivum* and *Triticum durum* growing in the Mediterranean region has not been used in this assessment.

The basis of the model used for calculating phytotoxic ozone doses is the calculation of an instantaneous stomatal conductance  $g_{sto}$  proposed by (Jarvis, 1976) and modified by (Emberson et al., 2000b) defined from following equation:

$$g_{sto} = g_{max} * [\min(f_{phen}, f_{O3})] * f_{light} * \max\{f_{min}, (f_{temp} * f_{VPD} * f_{sw})\}$$

where  $g_{sto}$  and  $g_{max}$  (species -specific maximum value for the stomatal conductance) are measured in  $\text{mmol O}_3 \text{ m}^{-2} \text{s}^{-1}$  of Projected Leaf Area (PLA). Parameters  $f_{phen}$ ,  $f_{O3}$ ,  $f_{light}$ ,  $f_{temp}$ ,  $f_{VPD}$ ,  $f_{sw}$  and  $f_{min}$  are expressed as relative proportions of  $g_{max}$ , taking values between 0 and 1. These functions allow taking into account the influence on stomatal conductance of irradiance ( $f_{light}$ ), temperature ( $f_{temp}$ ), water vapor deficit at leaf level ( $f_{vpd}$ ), soil moisture ( $f_{sw}$ ), the phenology for the different stage of growing ( $f_{phen}$ ) and the influence of ozone on stomatal flux by promoting premature senescence ( $f_{O3}$ ).  $f_{min}$  is the minimum relative value of stomatal conductance during daylight.

It is beyond the scope of the present report to further elaborate on the design of the stomatal conductance model. All the details are described in the Modelling and Mapping Manual (CLRTAP, 2017), providing a synthesis of appropriate values of all those parameters defining the stomatal conductance modifying functions for several crop, tree and grassland species.

The hourly stomatal conductance is subsequently accumulated over the growing season of the species being considered. For wheat, the accumulation period is defined for each year using the effective temperature sum in °C for days in excess of 0 °C. For the timing of mid-anthesis we follow the recommendation of the manual which is estimated by starting at the first date after 1 January when the temperature exceeds 0°C, or 1 January if the temperature exceeds 0 °C on that date. The mean daily temperature is then accumulated (temperature sum), and mid-anthesis is estimated to be a temperature sum of 1075 °C days for bread wheat. The total accumulation period during which wheat is sensitive to ozone exposure is 200 °C days before mid-anthesis (mid-point in flowering) to 700 °C days after mid-anthesis.

The soil moisture is also a sensitive parameter in the calculation of the POD. We use the Soil Moisture Index (SMI) using the EMEP methodology (Simpson et al., 2012), which is also described in the Scientific Background Document B on the ICP vegetation website<sup>1</sup>. It is computed using the soil moisture variable available from a meteorological model and represents the water content in  $\text{m}^3$  of water per  $\text{m}^3$  of ground (therefore as unitless as  $\text{m}^3/\text{m}^3$ ) in the 10-40 centimeters of the ground. The SMI is calculated from the soil moisture, the permanent wilting point and the field capacity which are taken from JRC database soil hydraulic properties maps (2016) for Europe<sup>2</sup>. SMI varies between 1 for field capacity to 0 at wilting point. In the present report, the meteorological parameters used to compute the soil moisture index and temperature accumulation are obtained from the same meteorological fields as those used to drive the Chemistry Transport Model simulations, i.e. the WRF model (Skamarock et al., 2008) as implemented for the IPSL-INERIS member of the Eurocordex reanalysis (Jacob et al., 2013) and used in the Eurodelta-Trends Project (Colette et al., 2017a), see Section 3.2.3. For this analysis, all wheat growing areas are considered rainfed i.e. without irrigation.

<sup>1</sup> <https://icpvegetation.ceh.ac.uk/publications/documents/ScientificBackgrounddocumentBNov17v2.pdf>

<sup>2</sup> <https://esdac.jrc.ec.europa.eu/content/maps-indicators-soil-hydraulic-properties-europe>

Once all those variables are computed, we can calculate the stomatal flux of ozone ( $F_{sto}$ ) based on the assumption that the concentration of ozone at the top of the canopy represents a reasonable estimate of the concentration at the upper surface of the laminar layer for a sunlit upper canopy leaf.  $F_{sto}$  is calculated according the Modelling and Mapping methodology, thus the fraction of the ozone taken up by the stomata is given using a combination of atmospheric ozone concentrations ( $c(z_i)$ ) and the stomatal conductance, the external leaf, or cuticular, resistance and the leaf surface resistance.

$$F_{sto} = C(z_1) * \frac{1}{r_b + r_c} * \frac{g_{sto}}{g_{sto} + g_{ext}}$$

The  $1/(r_b+r_c)$  term represents the deposition rate to the leaf through resistances  $r_b$  (quasi-laminar resistance) and  $r_c$  (leaf surface resistance),  $g_{ext}$  is the cuticular conductance.

$r_b$  is defined at leaf level according to (McNaughton and Van den Hurk, 1995) using use the cross-wind leaf dimension L [m] and the wind speed at height  $z_1$ ,  $u(z_1)$ . And  $r_c$  is simply defined as follow:

$$r_b = 1.3 * 150 * \sqrt{\frac{L}{u(z_1)}} ; \quad r_c = \frac{1}{g_{sto} + g_{ext}}$$

Where  $g_{ext}$  is simply scaled to  $1 / 2500$  in  $(\text{m s}^{-1})$  for consistency with the EMEP deposition modules “big-leaf” external resistance.

Then, hourly averaged stomatal O<sub>3</sub> fluxes ( $F_{sto}$ ) in excess of a threshold Y are accumulated over a species or vegetation-specific accumulation period using the following equation:

$$\text{POD}_Y = \sum [(F_{sto} - Y) \cdot (3600 / 10^6)] \text{ (mmol m}^{-2} \text{ PLA)}$$

Where the value Y ( $\text{nmol m}^{-2} \text{ PLA s}^{-1}$ ) is subtracted from each hourly averaged  $F_{sto}$  ( $\text{nmol m}^{-2} \text{ PLA s}^{-1}$ ) value only when  $F_{sto} > Y$ , during daylight hours (when global radiation is more than  $50 \text{ W m}^{-2}$ ). The value is then converted to hourly fluxes by multiplying by 3600 and to mmol by dividing by  $10^6$  to get the stomatal O<sub>3</sub> flux in  $\text{mmol m}^{-2} \text{ PLA}$ . For the wheat and other crop species Y = 6 ( $\text{nmol O}_3 \text{ m}^{-2} \text{ PLA s}^{-1}$ ).

Once the POD<sub>Y</sub> has been calculated, the following response function for wheat is applied (Grünhage et al., 2012, and Figure 2):

$$\text{Grain yield (\%)} = 100.3 - 3.85 \text{ POD}_6 \text{SPEC}$$

And the wheat yield loss is calculated as for AOT40:

$$(1 - \text{relative yield}) * \text{yield}$$

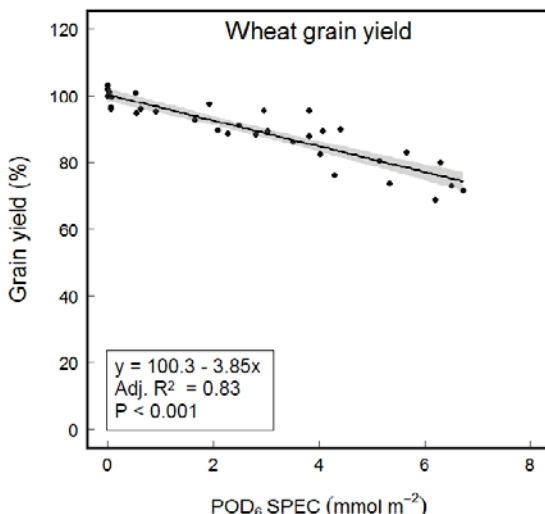


Figure 2: Dose-response function for wheat yield (in percentage of grain yield) and stomatal O<sub>3</sub> flux (POD<sub>6</sub>SPEC) for the wheat flag leaf based on five wheat cultivars from four European countries (Belgium, Finland, Italy, Sweden). The grey area indicates the 95%-confidence interval (Gründhage et al., 2012).

### 2.1.3 Vertical downscaling

Ozone exhibits an important vertical gradient close to the ground, in part because of deposition to and uptake by vegetation but chemical reaction with precursors emitted close to the surface also play a role in this gradient. This can lead to inconsistencies when comparing monitors with differing inlet height which ranges from 1.5 to 4 m according to the 2008 Directive (EC, 2008), or 3-5 m at EMEP sites<sup>3</sup> (CLRTAP, 2017).

The vertical gradient between 5 m and 1 m (representative height of the wheat canopy) is about 10% (Table III.7 of (CLRTAP, 2017)). Because of using thresholds, this gradient can have very large impact on the ozone metrics, an example is cited in (Mills et al., 2018) with AOT40 values decreasing from 16323 to 10800 ppb.hour (or a 35% decrease) when a downscaling from 5 m to 1 m is applied.

In order to comply with recommendations of the Modelling and Mapping Manual (CLRTAP, 2017), we apply such a downscaling to compute POD<sub>6</sub>SPEC for wheat. We use the approach detailed in (Tuovinen and Simpson, 2008). The technique consists of computing the ozone deposition using a similar formulation as used in Chemistry Transport Model with a roughness sublayer above an aerodynamically rough surface. The only difference is that here we compute that correction offline, i.e. after the CTM has completed the simulation.

For the observations, we lack precise information on the inlet height at individual monitoring station and therefore assume a 3 m height. For the models, we use the information provided by the EDT modelling groups (See Section 3.2.3). Some CTMs provide ozone estimates which already account for this vertical downscaling (EMEP and MATCH, where the representative height is 3 m, while it is 2.5 m for LOTOS-EUROS), while others provide the first model level (centered at 10 m and 20 m in CHIMERE and MINNI, respectively).

For AOT40, but also the other ozone metrics discussed in the validation (ozone annual mean and summertime peaks), we deliberately ignore this vertical downscaling. This is for consistency with other model evaluation studies, where it is considered that such a downscaling should remain the responsibility of modelers. This choice also ensures consistency with the AOT40 maps developed by the European Topic Centre on Air Quality and Climate Change Mitigation (ETC/ACM) which will be used for

<sup>3</sup> EMEP Manual, [https://www.nilu.no/projects/ccc/manual/documents/03\\_9-Determination%20of%20ozone.htm](https://www.nilu.no/projects/ccc/manual/documents/03_9-Determination%20of%20ozone.htm)

comparison purposes (Horálek et al., 2012). Those ETC/ACM maps are produced with a geostatistical data fusion process relying on ozone surface observations and chemistry-transport model results (EMEP in this case), as well as other explanatory variables (orography, meteorology, landuse etc.).

## 2.2 Inputs data

### 2.2.1 Crops

The localization of wheat fields over Europe was obtained from the United Nations' Food and Agriculture Organization database of harvested area of both rain-fed and irrigated wheat for year 2000<sup>4</sup>, as well as the corresponding yields (in kt). This information is available at a 0.08 degree resolution (or about 10km), which is considered satisfactory given the relatively large scale of ozone episodes, which are also estimated in the present report from model results at 25km resolution (see section 3.2.3). The reference year for those wheat production estimates is 2000, which is an appropriate mid-point for the trend assessed over 1990-2010. Using a single production estimate for the whole time period allows isolating the impact of ozone exposure on crop yields by neglecting other sources of fluctuation. For the present assessment, the soil moisture index approach is considered throughout Europe, whereas it could be corrected for artificially irrigated areas. The rationale for this choice is that we could only retrieve total wheat production over Europe without distinction between rain-fed and irrigated making irrelevant an attempt to differentiate the corresponding yield losses. A consequence may be an underestimation of the POD in the area where irrigated wheat crops are important.

The map of wheat yields in 2000 is shown in Figure 3 and the corresponding wheat production totals per country are provided in the first column of Table 2 .

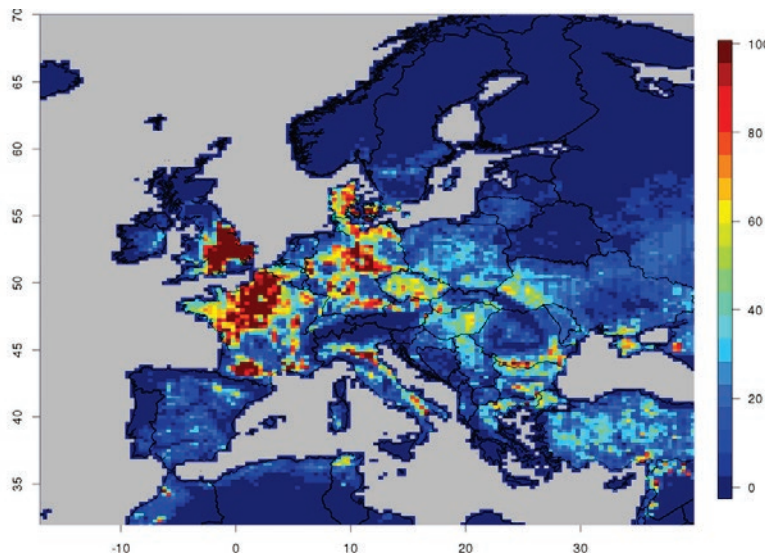


*Figure 3: Map of wheat production (both rain fed and irrigated crops) over Europe for 2000 (kt/gridcell), source: UN FAO database of yield and production by harvested area of rain-fed and irrigated wheat for year 2000.*

### 2.2.2 Observations

Chemistry Transport Models are particularly well suited to assess air pollution impacts because of their comprehensive geographical coverages whereas observations are only available at point locations. There

---

<sup>4</sup> <http://www.fao.org/nr/gaez/about-data-portal/agricultural-suitability-and-potential-yields/en/>, accessed 20180803

is however a need to assess the capabilities of the models. To perform this evaluation, we rely on the EMEP observations, which are available over a long timeperiod and therefore particularly well suited for trend assessments. EMEP monitoring stations are also relevant to evaluate the models with regard to agricultural exposure since they are typically rural background sites.

In the present report, we rely on a subset of EMEP data that were selected for their completeness and reliability to perform a trend assessment. The dataset of the TFMM Trend Report (Colette et al., 2016) is used here. The map of selected stations is provided in Figure 4, which illustrates the important bias in the representation of the network, which lacks monitoring stations to assess long-term trends in Mediterranean areas where ozone pollution is rather high.

These hourly ozone observations are used to compute several indicators that will be compared directly to chemistry transport models: ozone annual mean, summertime peaks (represented here with the 4<sup>th</sup> highest annual maximum daily eight-hour mean: 4MDA8), and AOT40. We also extract meteorological and soil moisture information at the station location from a mesoscale meteorological model (see Section 3.2.3) in order to compute POD<sub>6</sub>SPEC at the EMEP station location using observed hourly ozone.

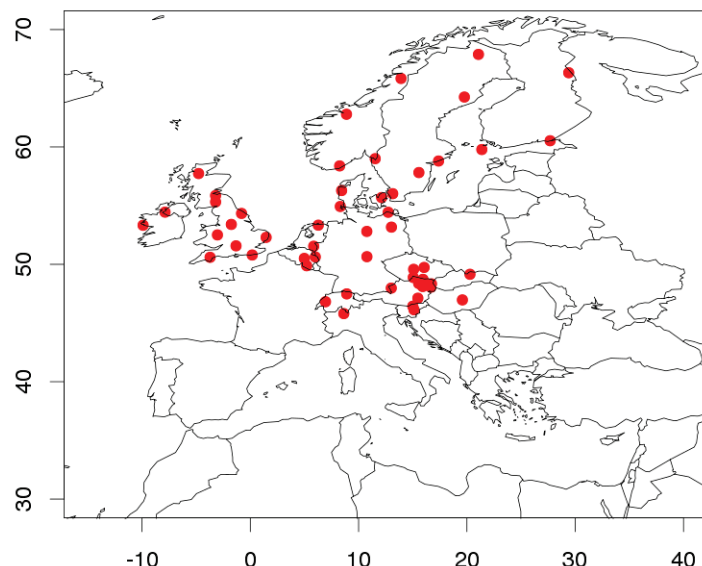


*Figure 4: EMEP stations where ozone data are temporally dense enough to assess long-term trends (available for at least 75% of the years over 1990-2012 and 75% of each year), source: TFMM 2016, (Colette et al., 2016).*

### 2.2.3 Modelling: Eurodelta-Trends multi model ensemble

A multi-model trend ensemble was recently compiled by the TFMM under the LRTAP Convention to explore the ability of regional CTMs in capturing air pollution trends in Europe. A complete description of the Eurodelta-Trends modelling exercise is available in (Colette et al., 2017a). A report including a validation of the Eurodelta-Trend (EDT) ensemble was also published in 2017 by ETC/ACM (Colette et al., 2017b).

The EDT exercise covered the period 1990-2010. The year 1990 was chosen because it is used as reference for the initial Gothenburg Protocol of 1999<sup>5</sup>, while the last year was chosen based on the availability of underlying forcing data (emission, boundary conditions and meteorology) when the

<sup>5</sup> Gothenburg Protocol to Abate Acidification, Eutrophication and Ground-level Ozone, [http://www.unece.org/env/lrtap/multi\\_h1.html](http://www.unece.org/env/lrtap/multi_h1.html)

modelling exercise was initiated. The modelling domain covers the European region ( $17^{\circ}\text{W}$  to  $39.8^{\circ}\text{E}$  and  $32^{\circ}\text{N}$  to  $70^{\circ}\text{N}$ ) and the model resolution is  $0.25^{\circ} \times 0.4^{\circ}$  of latitude  $\times$  longitude, which in Europe is approximately 25 km.

All models use identical trends in anthropogenic emissions. The International Institute for Applied Systems Analysis (IIASA) computed the anthropogenic emissions with the GAINS model (Greenhouse gas – Air pollution Interactions and Synergies, <http://gains.iiasa.ac.at>), as part of the ECLIPSE FP7 project (Evaluating the Climate and Air Quality Impacts of Short-Lived, <http://eclipse.nilu.no>), and provided them to the EDT study. More details on these emissions can be found in (Amann et al., 2012) and (Klimont et al., 2017). A single source of chemical boundary conditions is used by all CTMs. It consists of a simplified version of those used in the standard EMEP MSC-W model (Simpson et al., 2012), and it is based on in situ observation trends, in particular at the Mace-Head observatory, in Ireland. A common source of meteorological forcing was provided based on a dynamic downscaling of ECMWF (European Centre for Medium-Range Weather Forecasts) re-analyses with the WRF model (Stegehuis et al., 2015). The other processes are model dependent, including on-line computation of biogenic emissions.

### 3 Results

#### 3.1 Model validation

A comparison between EDT models and observations for ozone annual mean, summertime peaks (4MDA8 (Colette et al., 2016)); and as ozone crop impact indicators AOT40 and POD<sub>6</sub>SPEC are shown in Figure 5 and Figure 6, respectively. For those comparisons, we use an interpolation of the modelled ozone fields at the location of the EMEP monitoring stations. Since the selected stations are limited to the subset offering a comprehensive temporal coverage, their location is strongly biased towards central and northern Europe (see Figure 4). It should therefore be noted that the comparison is not representative of Mediterranean areas of Europe.

For the comparison between observed and modelled annual ozone mean, summertime peaks and AOT40, no vertical downscaling of observations was applied following the usual practices. It is only for the comparison of POD<sub>6</sub>SPEC that downscaling is taken into account, assuming a sampling height of ozone at 3 m and canopy height of 1m.

In order to provide a brief but comprehensive overview of the results, in Figure 5 and 6 we show time series and average trends for spatial composites taking the average of all EMEP stations for each year for either the observations, or the individual models, or the median ensemble of all models.

Table 1 we provide the trend and related uncertainty for each of the four ozone metrics, and three time periods: 1990 to 2000, 2000 to 2010, and 1990 to 2010. The trend is computed from the Sen-Theil slope, using either the median of the trend at individual stations or the trend of the composite time series over all stations as displayed in Figure 5 and 6. For the uncertainty, we provide the standard deviation of the trend at individual stations, as well as the p-value of the composite time series over all stations.

For the observations, there is a slight increase in annual mean ozone in 1990-2010 ( $+0.22 \mu\text{g}/\text{m}^3/\text{yr}$  for the average time series throughout Europe), and the trend is statistically significant (with the Mann-Kendall test and a 0.05 threshold). In the median ensemble of all EDT models, a very small non-significant decrease is found ( $-0.05 \mu\text{g}/\text{m}^3/\text{yr}$ ) and most of the models and the ensemble overestimate annual O<sub>3</sub> annual means. These features are well illustrated on the composite time series of Figure 5 and the statistics are summarized in Table 1. The discrepancy between models and observation is mainly found for the earlier time period (1990 to 2000), whereas the agreement is much better between 2000 and 2010 with non-significant decreasing trends for annual mean observed and modelled values at  $-0.16 \mu\text{g}/\text{m}^3/\text{yr}$  and  $-0.24 \mu\text{g}/\text{m}^3/\text{yr}$ , respectively. The spatial variability is high, the median of observed trends

of ozone annual mean between 1990 and 2010 across the 53 available European stations is  $0.13 \mu\text{g}/\text{m}^3/\text{yr}$ , but its standard deviation is 0.29, indicating that there are both increasing and decreasing trends depending on the location. The annual ozone mean is actually the ozone indicator that is less well captured by the models, as can be seen in the larger spread of the individual modelled time series compared to any of other indicators used.

For summertime ozone peaks, the models capture the significant decreasing trend found in the observations, however with an overestimation of the downward trend. In the observations, the trend of the average time series over the EMEP network in 1990-2010 is  $-0.93 \mu\text{g}/\text{m}^3/\text{yr}$ , while in the ensemble of EDT models it is  $-2.11 \mu\text{g}/\text{m}^3/\text{yr}$ . This overestimation of the downward trend in the models occurs also for both the 1990-2000 and 2000-2010 time periods. The overestimation is lower for the median trend in the 2000-2010 time period, indicating that the composite is heavily influenced by a few stations where the models underperform. The spread of EDT models is smaller for ozone peaks compared to ozone annual means, except for Lotos-Euros that stands out from the ensemble.

The trend of AOT40 and POD<sub>6</sub>SPEC indicators are provided in Figure 6. For AOT40, again the Lotos-Euros model stands out, while all the other models are relatively similar. In the observations, the AOT40 trend of the spatial composite in 1990-2010 is  $-53 \mu\text{g} \cdot \text{m}^{-3} \cdot \text{hour} \cdot \text{yr}^{-1}$  (not significant,  $p = 0.65$ ), while the models point towards a significant improvement of  $-417 \mu\text{g} \cdot \text{m}^{-3} \cdot \text{hour} \cdot \text{yr}^{-1}$  ( $p = 0.0003$ ). The agreement is much better for the 2000-2010 time period, with non-significant decreases in both the ensemble model ( $-479 \mu\text{g} \cdot \text{m}^{-3} \cdot \text{hour} \cdot \text{yr}^{-1}$ ) and observations ( $-513 \mu\text{g} \cdot \text{m}^{-3} \cdot \text{hour} \cdot \text{yr}^{-1}$ ), though in this case there is an underestimation in the decrease provided by the models.

For POD<sub>6</sub>SPEC, none of the trends are significant. This behavior illustrates that PODy is by construction influenced by both the trend in ozone background (annual mean) and peaks (4MDA8). The models underestimate the non-significant increase in the observations for the 1990-2010 time period, but the agreement is very good over the later time period (2000-2010).

To summarize, the models are “optimistic” in capturing ozone trends: overestimating the magnitude of decrease in ozone peaks and underestimating the magnitude of increase in ozone mean. For all indicators, the comparison between ensemble model and observations is much better in the second decade. It is the modelled overestimation in the early 1990s that contributes to overestimation of the downward trend over the 1990-2010 time period. Ozone annual mean are systematically overestimated by the models. It is also the case for the 1990-2000 decade for 4MDA8 and AOT40, whereas the agreement is better for the 2000-2010 decade. On the other hand, models estimate lower POD<sub>6</sub>SPEC than observations. Moreover, taking into account that wheat is irrigated in many areas (and POD<sub>6</sub>SPEC is therefore expected to be higher), models can be underestimating the O<sub>3</sub> effects in this analysis.

We should emphasize again however that this evaluation of the trends by means of comparison between models and observations is heavily biased geographically, with most stations being located in the northern part of Europe.

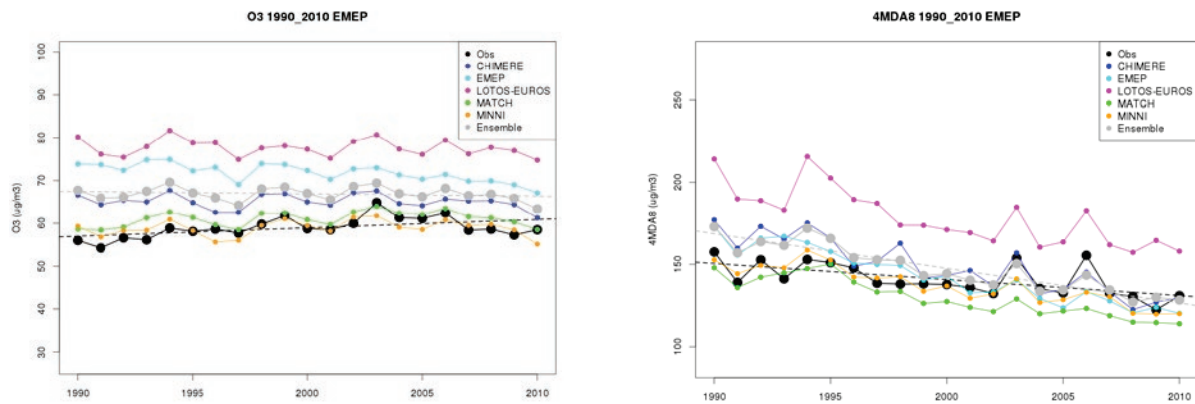


*Figure 5: Comparison of Eurodelta-Trends models interpolated at EMEP sites for ozone annual mean ( $\mu\text{g}/\text{m}^3$ ) and summertime maxima (as the average of daily max over June-July-August, in  $\mu\text{g}/\text{m}^3$ ). The straight dotted lines are for the fitted trend either in the observations (black) or in the model ensemble (grey).*

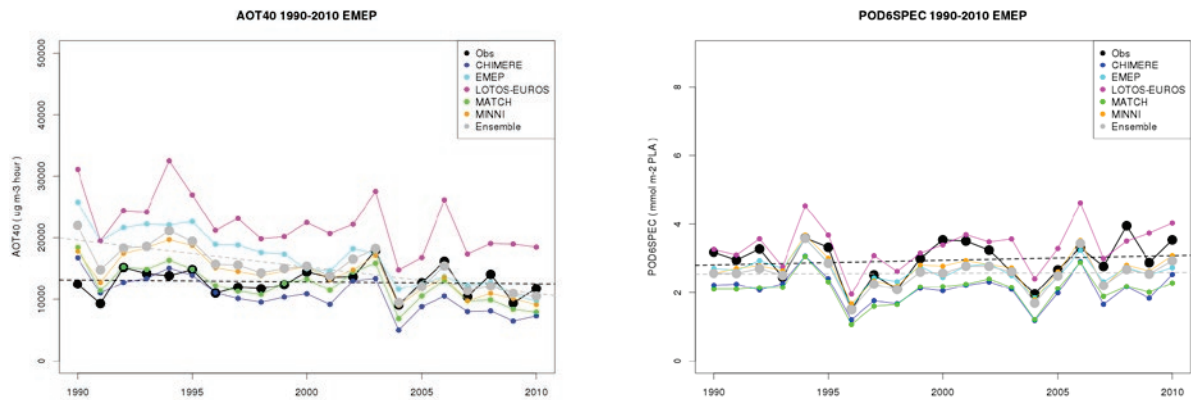


*Figure 6: Comparison of Eurodelta-Trends models interpolated at EMEP sites for AOT40 for agricultural crops ( $\mu\text{g} \cdot \text{m}^{-3} \cdot \text{hour}$ ) and POD<sub>6</sub>SPEC for wheat ( $\text{mmol} \cdot \text{m}^{-2} \cdot \text{PLA}$ ). The straight dotted lines are for the fitted trend either in the observations (black) or in the model ensemble (grey).*

*Table 1: Trends for the four ozone metrics (annual mean: O3 avg, summertime peaks: 4MDA8, AOT40 and POD<sub>6</sub>SPEC) over the three time periods considered (1990 to 2000, 2000 to 2010 and 1990 to 2010), for either the observations (OBS) or the Eurodelta-Trend median ensemble model (MOD). The number of selected stations is provided as well as the average observed or modelled indicator for each time period. The trends are given either as the median of individual trends at various stations or as the trend of the mean composite in Europe (as displayed in Figure 5 and Figure 6). The spatial variability of the trend is provided (std dev) as well as the significance of the trend in the composite (p-value), highlighted in green when lower than 0.05.*

Ozone Metric	Time Period	Number of stations	OBS/MOD	Average	median trend	std dev	composite trend	composite p-value
O3avg ( $\mu\text{g}/\text{m}^3$ )	1990_2000	44	OBS	57,3	0,418	0,564	0,364	0,013
		44	MOD	66,8	0,039	0,149	0,030	0,876
	2000_2010	53	OBS	60,0	-0,247	0,596	-0,164	0,350
		53	MOD	66,7	-0,288	0,138	-0,238	0,119
	1990_2010	53	OBS	58,9	0,126	0,292	0,224	0,032
		53	MOD	66,9	-0,065	0,124	-0,051	0,381
	4MDA8 ( $\mu\text{g}/\text{m}^3$ )	1990_2000	44	OBS	143,6	-1,570	2,241	-1,839
			44	MOD	158,8	-2,257	1,009	-2,612
		2000_2010	53	OBS	136,2	-1,000	1,456	-0,792
			53	MOD	136,7	-1,575	0,529	-1,603
		1990_2010	53	OBS	140,7	-0,848	1,035	-0,934
			53	MOD	147,6	-1,965	0,681	-2,108
AOT40 ( $\mu\text{g} \cdot \text{m}^{-3} \cdot \text{hour}$ )	1990-2000	34	OBS	13105,7	82,8	525,53	22,1	0,876
		34	MOD	18070,4	-461,9	464,16	-555,6	0,087
	2000-2010	53	OBS	14177,5	-276,3	514,82	-513,4	0,161
		53	MOD	14236,7	-499,0	251,19	-478,9	0,062
	1990-2010	41	OBS	12881,7	-44,6	170,81	-52,5	0,651
		41	MOD	15292,1	-457,6	248,46	-416,6	0,000
POD <sub>6</sub> SPEC (mmol.m <sup>-2</sup> .PLA)	1990-2000	34	OBS	2,9	0,000	0,132	-0,013	0,876
		34	MOD	2,7	-0,031	0,111	-0,021	0,350
	2000-2010	53	OBS	3,4	0,000	0,133	0,007	1,000
		53	MOD	2,9	-0,008	0,090	0,007	1,000
	1990-2010	41	OBS	2,9	0,000	0,087	0,018	0,526
		41	MOD	2,6	-0,001	0,070	0,004	0,786

## 3.2 Maps

### 3.2.1 AOT40

Figure 7 presents a comparison of AOT40 computed from the EDT ensemble and from the data fusion of ETC/ACM (See section 3.1.3), which is used in EEA annual air quality report such as (EEA, 2018). Two years of overlap between the ETC/ACM and EDT maps are provided (2009 and 2010).

There is a notable difference in the methodology of both approaches: in the ETC/ACM maps, observations are fused with the underlying (EMEP) model ensuring a good consistency between both. For EDT, it is rather an evaluation since measurements are merely superposed on the modelled maps to

indicate where the models under estimate the observations. No attempt was made to correct the EDT models on the basis of observations although it can be done.

The number of stations is also very different. For ETC/ACM all Airbase stations are included and for the EDT comparison only with the EMEP stations available over a long time-period (that were used for the time series of Figure 6) are shown.

The spatial pattern and order of magnitude is similar: in both cases, the maximum AOT40 values are found in Southern Europe. There are however substantial differences between 2009 and 2010. In 2010, according to ETC/ACM, the highest AOT40 values are found over South-Eastern France and Northern Italy, with also high values in Spain and to a lesser extent some areas in Germany. EDT captures the same variability, however with a systematic underestimation of the highest levels that also appears when comparing EDT and observations for high exposure stations (the discrepancy is lower at stations where observed AOT40 are low or moderate). The underestimation for 2010 can also be seen in the average time series of AOT40 in Figure 6. This bias does not appear for 2009 (neither in the time series nor in the maps, where observations are dense enough), for example, the higher levels for that year in Southern Italy are found both in the EDT and ETC/ACM maps.

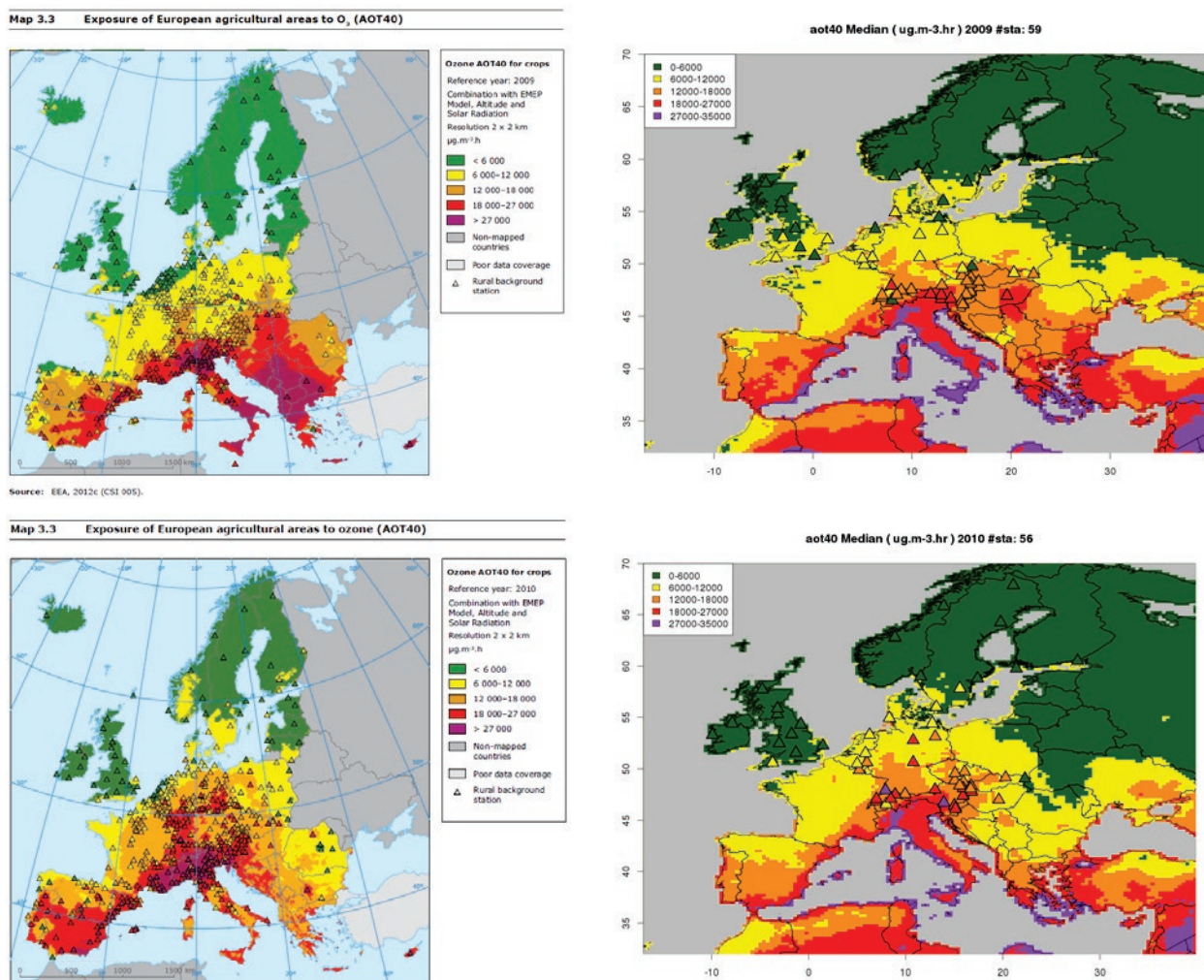


Figure 7: AOT40 ( $\mu\text{g.m}^{-3} \text{hr}$ ) for 2009 (top) and 2010 (bottom) in the 2012 and 2013 EEA's Air Quality Report (EEA, 2012, 2013) (left) and in the median model of the EDT ensemble (right)

A closer look at individual models in the EDT ensemble shows that all Chemistry-Transport Models involved in EDT display similar features, except the LOTOS-EUROS model, which shows substantially

higher values for ozone indicators than the other CTMs (Figure 8). The last panel provides a map of the coefficient of variation (standard deviation in the ensemble divided by the mean). The largest variation is found over the north-eastern part of the domain, where AOT40 levels are low.

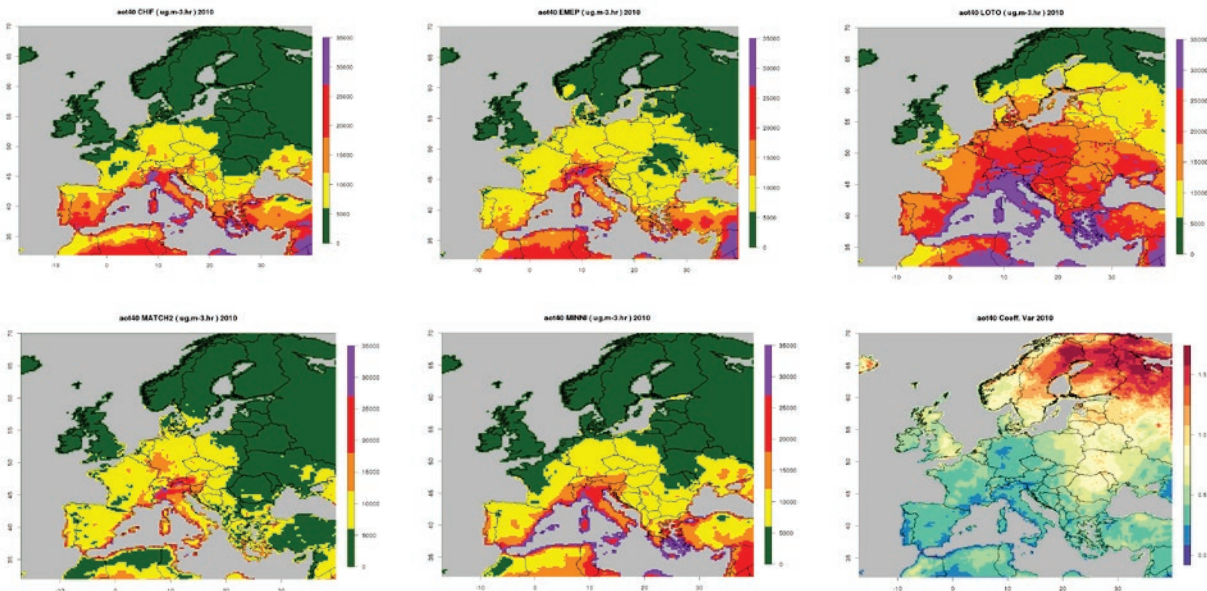


Figure 8: AOT40 ( $\mu\text{g m}^{-3} \text{ hr}$ ) for 2010 according to individual EDT models (Chimere, EMEP/MSC-W, Lotos-Euros, MATCH, MINNI), last panel: coefficient of variation.

### 3.2.2 $\text{POD}_6\text{SPEC}$

Figure 9 presents a comparison of  $\text{POD}_6\text{SPEC}$  derived with the methodology described in 3.1.2 applied to the EDT ensemble model versus the EMEP computation available in (Mills and Harmens, 2011) for the year 2000. The order of magnitude of both  $\text{POD}_6\text{SPEC}$  estimates are similar and depending on the locations, no clear over or underestimating bias appears. There is however an important difference as the impact of soil moisture on  $\text{POD}_6\text{SPEC}$  was not included in the (Mills and Harmens, 2011) study. This has a strong impact in Hungary/Romania, where the well documented drought in 2000 (Holobaca et al., 2003) leads to null  $\text{POD}_6\text{SPEC}$  values inland in our estimate with EDT that accounts for soil moisture (while important levels remain close to the coast).

We also notice here by comparing qualitatively Figure 7 and Figure 9, as pointed out in previous comparisons between AOT40 and  $\text{POD}_Y$ , that higher exposure is found over central and western Europe with  $\text{POD}_Y$ , while levels are usually lower in Southern Europe (Simpson et al., 2007).

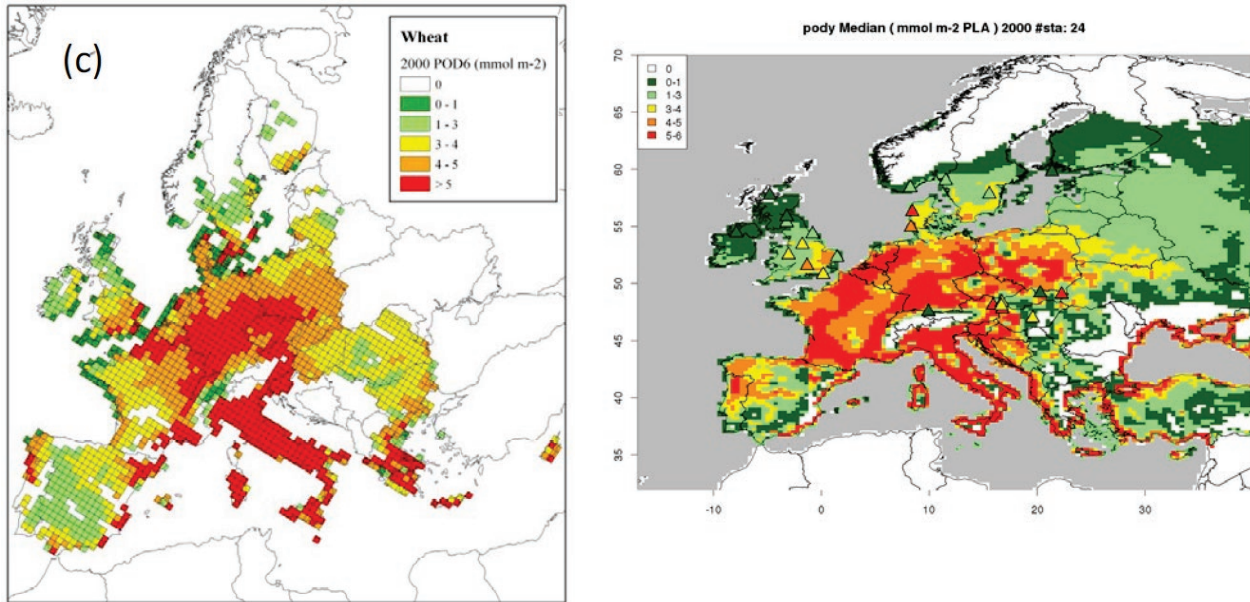


Figure 9:  $POD_6$ SPEC ( $\text{mmol m}^{-2}$  PLA) for 2000 estimated with the EMEP model (left, Fig 3.3. of (Mills and Harmens, 2011)), and the EDT median (right). Note: Map on the left only shows  $POD_6$ SPEC in areas where wheat is grown.

Comparing the  $POD_6$ SPEC estimates of individual models for a given year (2000) in Figure 10 shows higher values for the Lotos-Euros and Match models, while the order of magnitude and geographical patterns are quite similar for the other models. The largest spread in the ensemble is found in large gradient areas, where  $POD_6$ SPEC values decrease rapidly, and therefore exposure is limited. Note that unlike in Section 4.2.1, the individual model maps are for 2000 for consistency with the median ensemble shown in Figure 9 which is compared to the published estimate of (Mills and Harmens, 2011).

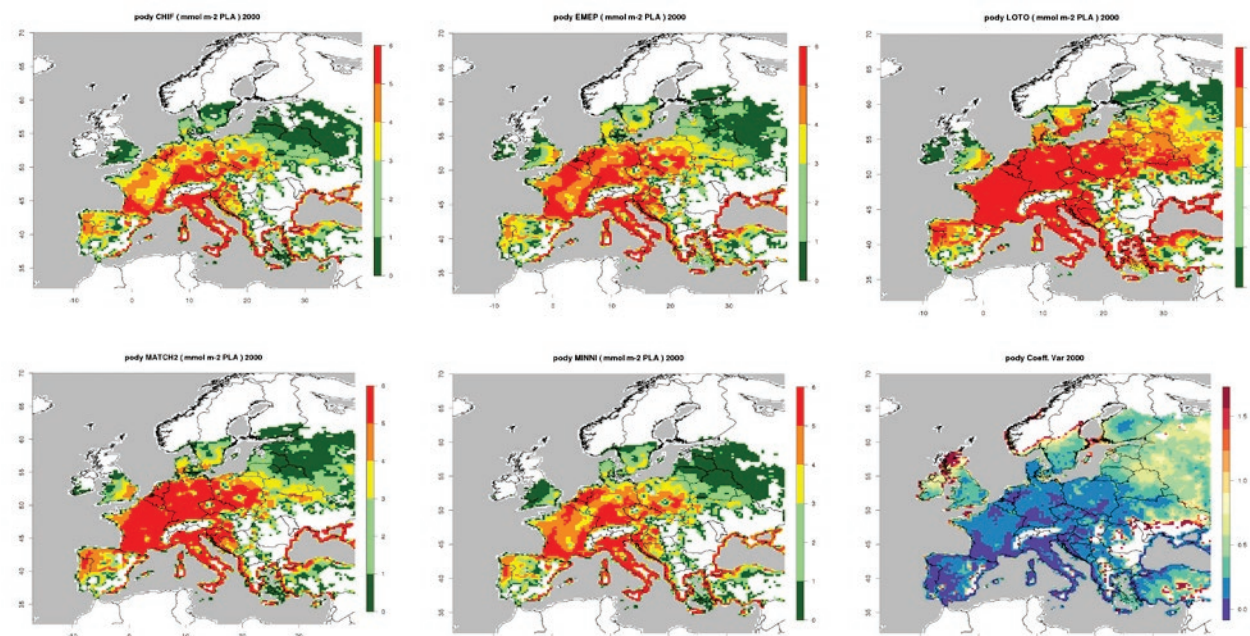


Figure 10:  $POD_6$ SPEC ( $\text{mmol m}^{-2}$  PLA) for wheat for 2000 according to individual EDT models (Chimere, EMEP/MSC-W, Lotos-Euros, MATCH, MINNI), last panel: coefficient of variation.

The comparison of the EDT maps of AOT40 and  $POD_6$ SPEC with estimates available in the literature (Mills and Harmens, 2011;EEA, 2013) indicate that the orders of magnitude are quite similar. There are quantitative differences, which were expected given the variety of methodologies used in the various assessments. Most importantly, we capture well the main qualitative difference between both metrics:

while AOT40 reaches maximum values in Mediterranean areas, especially in coastal areas and the Po-Valley, high POD<sub>6</sub>SPEC values are much more widespread with high values found in central Europe. The relatively low levels in Spain can be explained by the low sensitivity of POD<sub>6</sub>SPEC to the low soil moisture content during the growing season. However, these results should be taken cautiously since the specific parameterization of the stomatal conductance model adapted for wheat growing in Mediterranean areas has not been considered in this analysis.

### 3.3 Trends

#### 3.3.1 Map of Trends

The comparison of trends computed with both indicators for each grid cell provided in Figure 11 and 12 illustrates the larger relative decrease of ozone exposure derived with the AOT40 indicator compared to POD<sub>6</sub>SPEC. According to AOT40, the decline was larger in the 1990s than in the 2000s in France and Germany, whereas the opposite is true for Mediterranean countries. Significant trends (with a p-value for Mann-Kendall test below 0.05) are mostly found for decreases in AOT40, while there are very few areas where trends are significant for POD<sub>6</sub>SPEC.

Two factors may play a role in this difference between the trends found for AOT40 and POD<sub>6</sub>SPEC:

- Ozone trends differ depending on the metric being considered (Lefohn et al., 2017). For Europe for the period 1990-2010, a slight increase in ozone annual mean is observed, whereas ozone summertime peaks decreased (Colette et al., 2016; Simpson et al., 2014). For AOT40, only concentrations above 40 ppb (ca. 80 µg m<sup>-3</sup>) are accumulated to calculate the risk of wheat yield losses due to ozone. For POD<sub>6</sub>SPEC, concentrations as low as 20 ppb are included in the calculation of the risk (Scientific Background Document A, Modelling and Mapping Manual, 2017<sup>6</sup>). Therefore, the trend in POD<sub>6</sub>SPEC is more influenced by the trend in annual mean ozone, whereas the trend in AOT40 is relatively more influenced by the trend in peaks.
- Trends of the soil moisture index also play a role (Figure 13). An increase was found in the 1990s throughout Europe, which largely compensate the decreasing exposure to atmospheric ozone obtained with the AOT40 indicator. For the 2000s that increase was limited to Mediterranean and Balkan countries, where AOT40 exposure is high. When soil moisture increases, the plant can keep absorbing ozone, even during periods of mild drought, so that its exposure to ozone increases, as reflected with the POD<sub>6</sub>SPEC indicator. It should be noted that the comparison is limited here to two 10-year periods, which are obviously too short to draw robust conclusion on long-term climate trends. Coincidentally, the trends we find for soil moisture over a too short record are contradictory with the expected long-term drying in the future for Mediterranean areas (Spinoni et al., 2017; Hanel et al., 2018)<sup>7</sup>.
- Other factors could also play a role, such as temperature or vapor pressure deficit, which bears upon the length of the growing season and stomatal uptake of ozone (Andersson et al., 2017; Karlsson et al., 2017).

<sup>6</sup> <https://icpvegetation.ceh.ac.uk/publications/documents/ScientificBackgroundDocumentANov17.pdf>

<sup>7</sup> <https://www.eea.europa.eu/data-and-maps/indicators/water-retention-4/assessment>

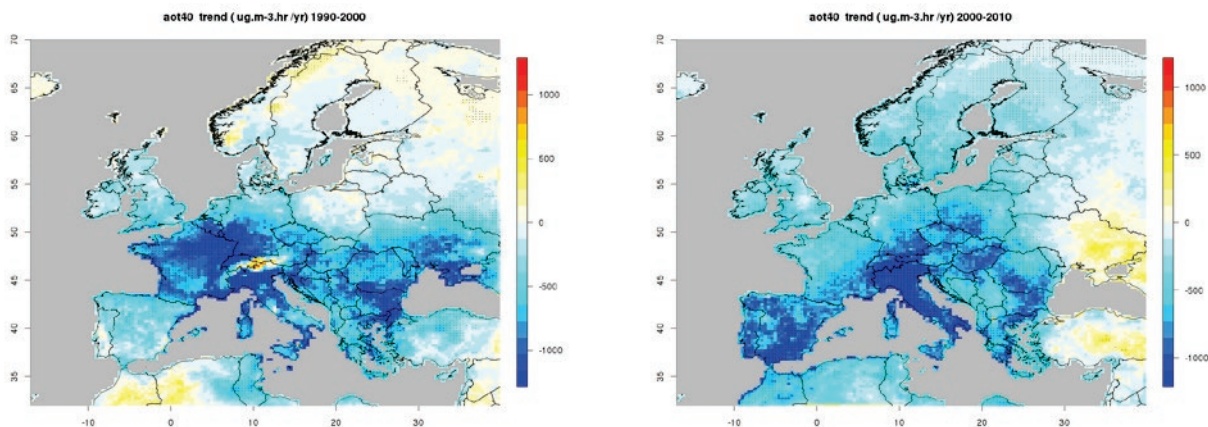


Figure 11: AOT40 trend ( $\mu\text{g.m}^{-3}.\text{hour.yr}^{-1}$ ) in 1990-2000 (left) and 2000-2010 (right) in the median of EDT models. The significance of the trend is indicated with dots where the Mann-Kendall test yields a  $p$ -value below 0.05.

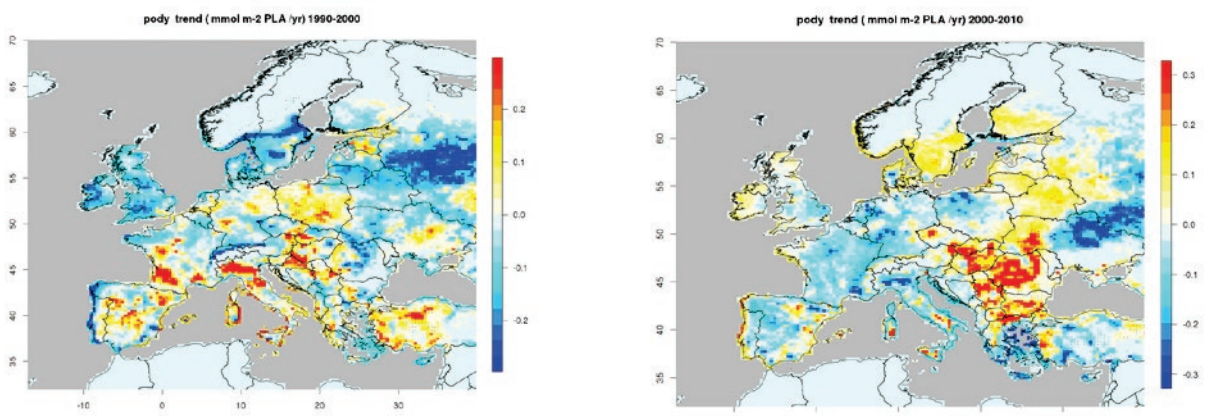


Figure 12: POD<sub>6</sub>SPEC trend ( $\text{mmol m}^{-2} \text{PLA yr}^{-1}$ ) in 1990-2000 (left) and 2000-2010 (right) in the median of EDT models. The significance of the trend is indicated with dots where the Mann-Kendall test yields a  $p$ -value below 0.05.

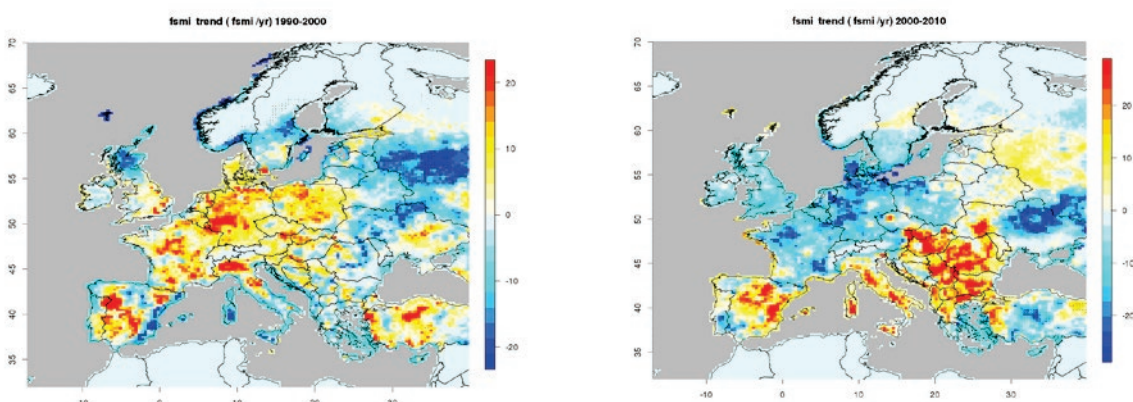


Figure 13: Accumulated Soil Moisture Index (unitless) trend in 1990-2000 (left) and 2000-2010 (right) in the median of EDT models. The significance of the trend is indicated with dots where the Mann-Kendall test yields a  $p$ -value below 0.05.

The trend maps also provide another opportunity to compare models and observations. The recent Tropospheric Ozone Assessment Report (TOAR), (Mills et al., 2018) published a map of trends over 1995-2014 for AOT40 for wheat (i.e. accumulated over May to July) reproduced here in Figure 12. The AOT40 definition differs slightly to the indicator used in our report since (Mills et al., 2018) used the CLRTAP indicator.

The trends of AOT40 reported in the TOAR assessment are very scattered, with a vast majority of non-significant trends. Only slightly more than 5% of the 357 European sites included in the assessment exhibit a significant decreasing trend. Referring back to the comparison between the EDT ensemble and observations in Section 4.1., Figure 14 confirms the risk that the EDT ensemble overestimates the magnitude of decrease in AOT40, especially in the 1990s. Even if the EDT experiment was designed to minimize the model uncertainties by relying on an ensemble of models to compensate for possible inaccuracies in individual participating models. However, all models used the same input data such as emission trends, which therefore can be responsible for the systematic bias in the trends.

Unfortunately, because of the uneven coverage of the monitoring network, this validation is heavily weighted by trends in Germany (and to a lesser extent, Austria, United Kingdom, and the Benelux). There are not enough stations in France, Spain, Italy and Central Europe to confirm whether this overestimation of decreasing trends in the models also occurs in those areas. And because (i) emission trends are reported by country, and (ii) ozone chemistry is non-linear, it is not possible to extrapolate the bias found over UK-Benelux-Germany to Mediterranean countries.

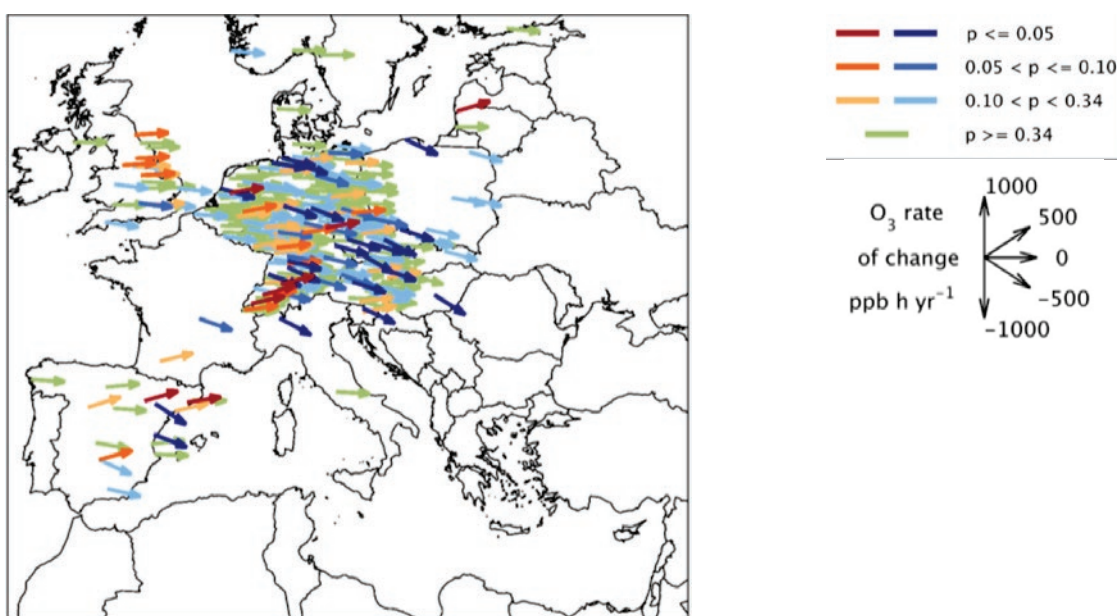


Figure 14: Observed trends in AOT40 for wheat over the 1995–2014 period from the TOAR report, source: (Mills et al., 2018) (Fig 21)

### 3.3.2 Trends of country-average AOT40 and $POD_6SPEC$

A comparison of country averaged AOT40 and  $POD_6SPEC$  is provided in Figure 15. Decreasing trends are found for both indicators for most countries in western Europe, although the decreasing trend is larger for AOT40. A very different behaviour is found for Scandinavian, Baltic and Mediterranean countries (except Greece), as well as a few central European countries (Austria, Hungary, Czech Republic and Slovakia) for reasons listed in Section 4.3.1.

The significance of the trend by country is indicated in the figure, when the Mann-Kendall statistic is below 0.05. It appears that while significant decreasing trends are found for AOT40, the trends are not significant for  $POD_6SPEC$  at the 0.05 levels. At a 0.1 level, we would conclude that  $POD_6SPEC$  trends are significant only in Cyprus, France, Germany, Luxemburg, United Kingdom (all showing a decline) and Macedonia (increase).

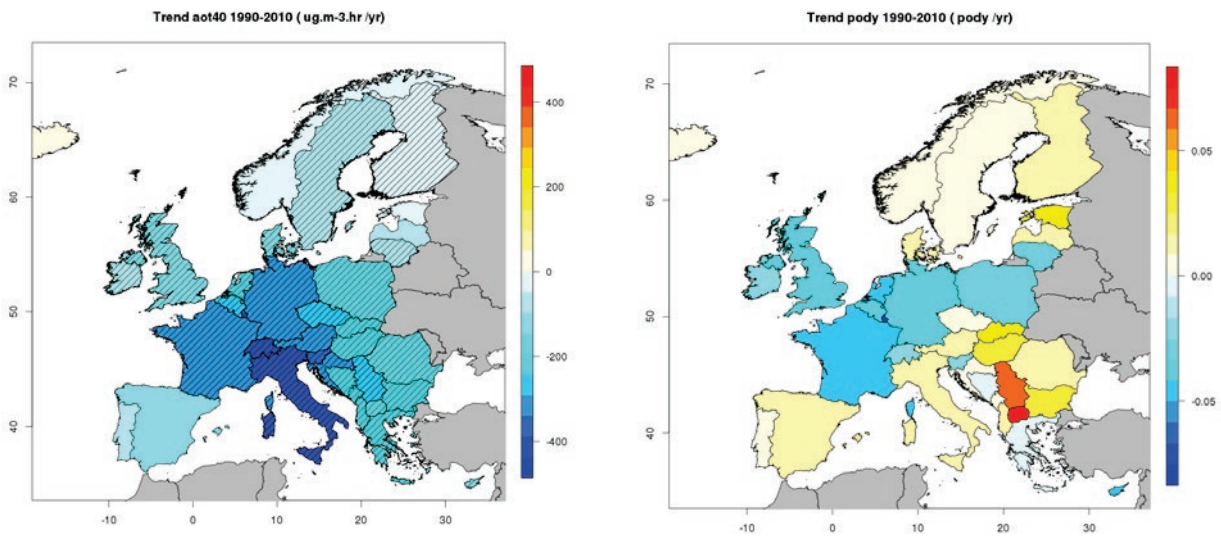


Figure 15: Trend in country averaged AOT40 and POD<sub>6</sub>SPEC over the period 1990-2010. Countries where the trend is significant are hatched.

### 3.3.3 Time series averaged over Europe for AOT40 and POD<sub>6</sub>SPEC

A pan-European composite of the country averages for both indicators is shown in Figure 16, marked as "EUR", for the following 37 countries: Albania (AL), Austria (AT), Belgium (BE), Bosnia and Herzegovina (BA), Croatia (HR), Cyprus (CY), Czech Republic (CZ), Denmark (DK), Estonia (EE), Finland (FI), France (FR), Germany (DE), Greece (GR), Hungary (HU), Island (IS), Ireland (IE), Italy (IT), Latvia (LV), Lithuania (LT), Liechtenstein (LI), Luxemburg (LU), the former Yugoslav Republic of Macedonia (MK), Malta (MT), Montenegro (ME), the Netherlands (NL), Norway (NO), Poland (PL), Portugal (PT), Romania (RO), Slovakia (SK), Slovenia (SI), Spain (ES), Serbia (RS), Sweden (SE), Switzerland (CH), and United Kingdom (UK).

The European composite was computed by weighting individual country averages by the area of the corresponding country. An alternative to producing a European average would be to weight individual countries by their wheat production, but then we would find an identical interannual variability as discussed in Section 4.4 devoted to the trends in yield losses. For complementarity, we therefore decided to use a surface weighting.

The average AOT40 for 2010 for those 37 European countries is 6,498  $\mu\text{g}/\text{m}^3.\text{hr}$ , which is in line with the representative average of AOT40 for wheat at 1418 European stations for the 2010-2014 period reported in the Tropospheric Ozone Assessment Report: 5,324 ppb.hr (std dev 2,884), i.e. about 10,648  $\mu\text{g}/\text{m}^3.\text{hr}$  (std dev 5,768) (Mills et al., 2018).

A decrease in AOT40 exposure is found, which is not reflected in terms of POD<sub>6</sub>SPEC. According to Section 4.3.2, this is mainly due to opposite AOT40 and POD<sub>6</sub>SPEC trends in Scandinavian, Baltic and Mediterranean countries (except Greece), as well as a few central European countries, where decreases are found for AOT40 whereas POD<sub>6</sub>SPEC slightly increases. As pointed out in 4.3.1, the underlying reason for these differences include (i) different sensitivity of AOT40 and POD<sub>6</sub>SPEC to changes in background/peak ozone (that exhibit contrasting trends), (ii) other meteorological factors that influence the length of the growing season and stomatal uptake of ozone.

For comparison, the time series in the eight largest wheat producing countries are also indicated in Figure 16. AOT40 is highest in Italy and Spain, whereas AOT40 is lowest in the United Kingdom. POD<sub>6</sub>SPEC is highest France, Germany, Poland, and Italy and lowest for the United Kingdom. For Spain, POD<sub>6</sub>SPEC is close to the European average.

It should be noted that the comparison to observations in Section 4.1 indicated a likely overestimation of the AOT40 decrease indicated by the models, whereas the trend in POD<sub>6</sub>SPEC indicated by the models was in agreement with observational trends. Even if such a comparison lacks geographical representativeness (with only few stations, mostly in Northern Europe, available for long-term comparison), we can hypothesize that the decrease of AOT40 over Europe presented here is an upper estimate and the actual declining trend is probably less.

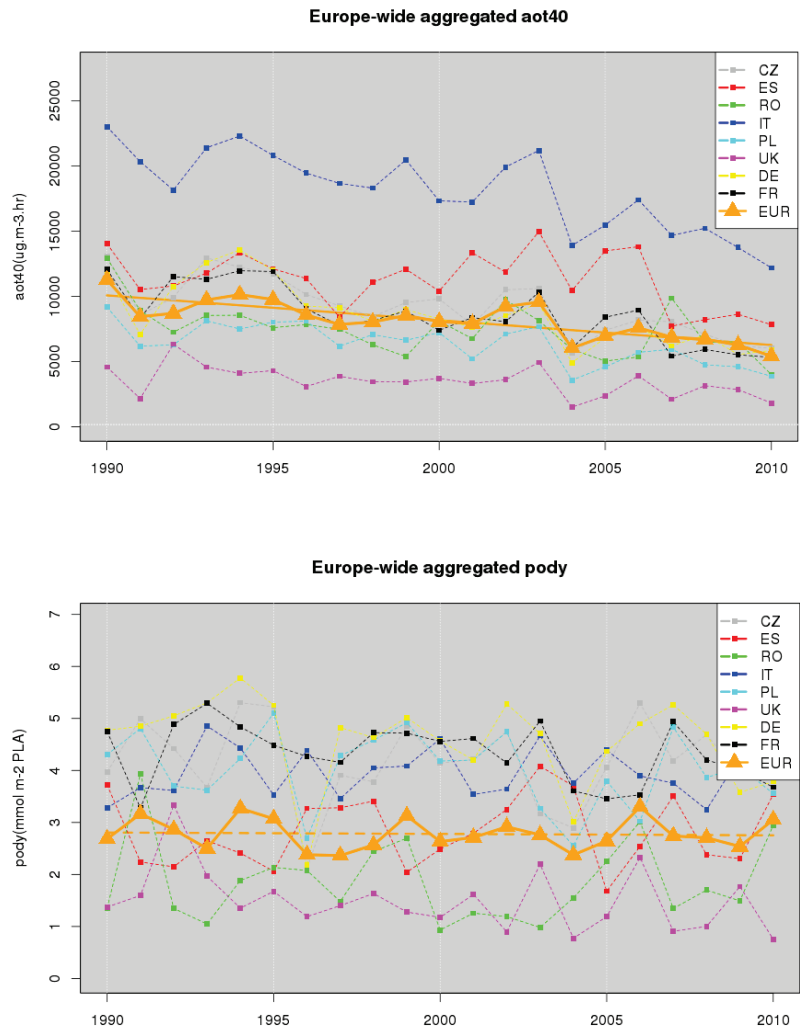


*Figure 16: AOT40 and POD<sub>6</sub>SPEC for wheat time series between 1990 and 2010 for Europe (surface-weighted) and the eight largest wheat producing countries. The straight orange line represents the linear fit of the European composite over the whole 1990-2010 period, dashed when non-significant.*

### 3.4 Loss

Using the exposure and dose-response functions introduced in Section 3.1, it is possible to assess the country average yield losses for wheat in Europe over the 1990-2010 time period. In order to focus on the impact of ozone on wheat, we decided to ignore other factors affecting the year to year variability in yield by using only the 2000 production estimates (Section 3.2.1).

A baseline check was performed by computing POD<sub>6</sub>SPEC in a CTM simulation where the ozone concentrations were re-calculated with all European Anthropogenic sources excluded. The corresponding impact on wheat crop yield was only 1.5% of the European production which, considering the uncertainties of such an assessment, is close enough to zero to conclude that the POD<sub>6</sub>SPEC metric is

selective for the purpose of our assessment, otherwise an offset should have been considered to calculate the impact of anthropogenic ozone alone (see Annex 1).

The time series of aggregated losses in wheat yield due to ozone derived from either AOT40 or POD<sub>6</sub>SPEC are provided in Figure 17, either for individual countries or aggregated over Europe. Since only 2000 wheat crop production data was used, the temporal variability at the country level is identical as the exposure/dose time series discussed in Section 4.3.3. However, the European aggregate differs because the country-level trends are now weighted by the production of the corresponding country.

The most striking feature is the statistically significant decrease of the detrimental impact of ozone on wheat yield when using AOT40, whereas the trend is not significant when using POD<sub>6</sub>SPEC.

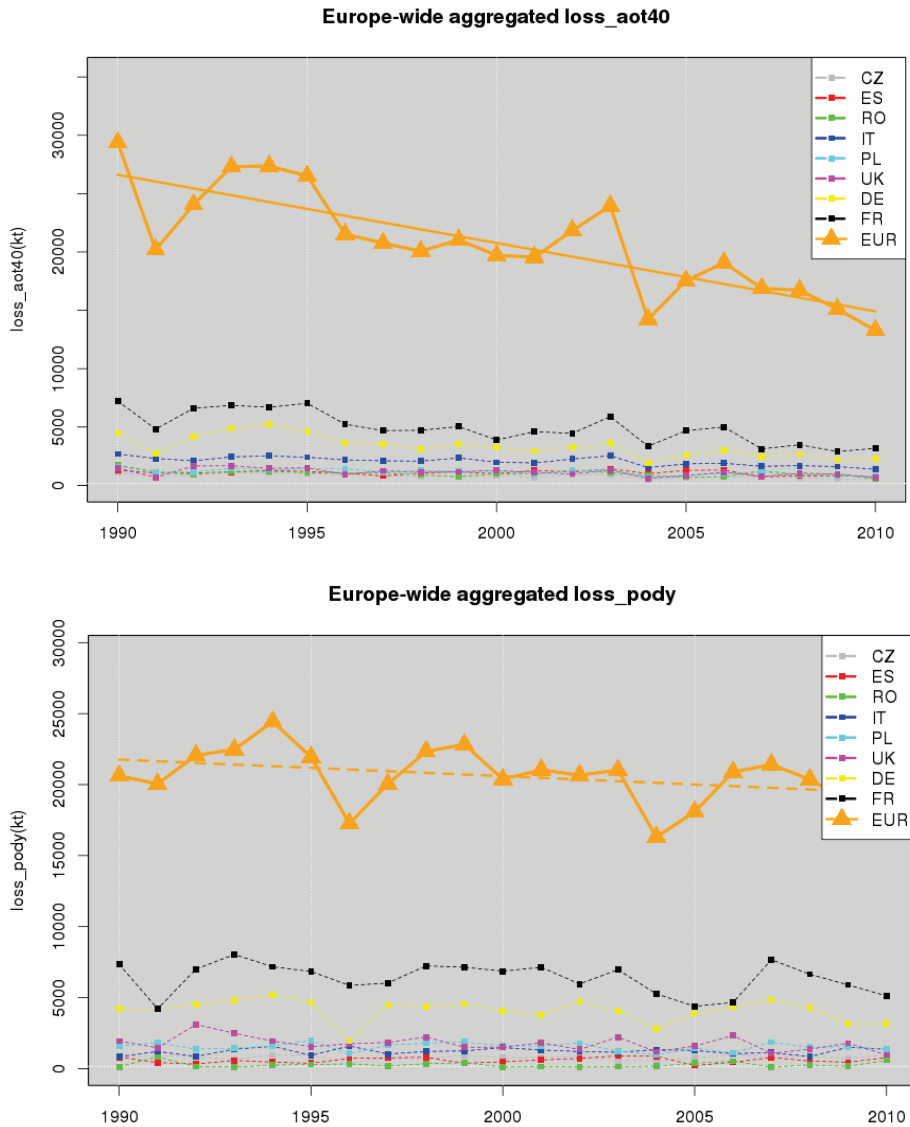


*Figure 17: Loss (kt) (derived from AOT40 and POD<sub>6</sub>SPEC for wheat) time series between 1990 and 2010 for Europe (surface-weighted) and the eight largest wheat producing countries. The straight orange line represents the fit of the ensemble for the trend over the whole 1990-2010 period, dashed when non-significant.*

A more detailed analysis can be performed when comparing the individual country values provided in Table 2 and Figure 18 for the 1990-2010 period and Table 3 and Figure 23 (both in Annex 2) for the 2000-2010 period. In those tables, we provide the fitted trends and their significance for both the whole 1990-2010 and 2000-2010 time periods. The values for the years 1990, 2000 and 2010 are also extracted from those fitted trends, in order to minimize the impact of interannual variability. As an example in Figure 17,

the yield loss for France using POD<sub>6</sub>SPEC varies strongly between 1990 and 1991 (7342kt versus 4210kt), using the linear fitted trend a more robust estimate can be provided (6899kt in Table 2).

Again, a very different behaviour is found for AOT40 and POD<sub>6</sub>SPEC. According to AOT40, the impact of ozone exposure on wheat yield in Europe decreased significantly from 18.2 to 10.2% between 1990 and 2010. Using POD<sub>6</sub>SPEC, a much less optimistic perspective is found since ozone impacts on wheat yield exhibited a non-significant decrease from 14.9 to 13.3%.

The values provided in Table 2 for individual countries are also represented as histograms in Figure 18 (sorted by total wheat production per country). The decrease of detrimental effect of ozone on crops between 1990 and 2010 ranged from 19 to 66% according to AOT40 and the decrease was statistically significant for almost all countries. In contrast, trends based on POD<sub>6</sub>SPEC are statistically significant for only two countries (increase in Macedonia and decrease in UK) and the relative changes range from a decrease of 54% to an increase of 159%.

As pointed out in Section 4.1 and 4.3.1 the comparison between models and observation indicate an overestimation of modelled decreasing AOT40 trends, especially in the 1990s. However, that comparison is mainly representative for Germany (and to a lesser extent, Austria, United Kingdom and the Benelux) because of the scarce monitoring network in other areas of Europe in the 1990s. Because all models suffer from the same bias, the underlying reason for this mismatch is probably due to trends in emission inventories. And since emission trends are reported by country, even if ozone has an obvious transboundary component, there is no reason to think that the models suffer from a particular bias in France, Poland, Italy, Romania Spain and Czech Republic (to name only the largest wheat producers).

However, the agreement between models and observations are better for the 2000-2010 period, for which the impacts are summarized in Table 3 and Figure 21 (Annex 1). For the year 2000, the European-wide negative impact of ozone on wheat yield is 13.9%, which is similar to estimates available in the literature: 13% (Mills and Harmens, 2011) - 14% (Pleijel et al., 2014). For the 2000-2010 decade, we also report a lack of statistical change of impact derived from POD<sub>6</sub>SPEC (from 13.9 to 13.3% yield loss), but for AOT40, the change in yield loss remains significant from 13.5% (2000) to 10.2% (2010).

**Table 2: Country averages or aggregated metrics and impacts: total wheat production (in kt), AOT40 (in  $\mu\text{g}/\text{m}^3.\text{hr}$ ) for 1990 and 2010, POD<sub>6</sub>SPEC (in  $\text{mmol m}^{-2} \text{PLA}$ ) for 1990 and 2010, AOT40 and POD<sub>6</sub>SPEC derived loss in wheat production (in kt) and % of the country production for 1990 and 2010 as well as annual trend between 1990 and 2010 (in kt/yr). A negative trend in ozone impacts on crops means an increase in crop production, the trend is considered significant when the indicated p-value is lower than 0.05. Increases are highlighted in red, decrease are highlighted in green. Instead of providing the actual indicator and loss for 1990 or 2010, we provide an estimate based on the linear fit of the trend for 1990 or 2010 to minimize the impact of interannual variability.**

Country	Wheat Production (kt)	AOT40 1990	AOT40 2010	POD6 1990	POD6 2010	Max Loss AOT40 1990 (kt)	AOT40 1990 (%)	Max Loss AOT40 2010 (kt)	AOT40 2010 (%)	Trend Loss AOT40 (kt/yr)	Trend Signif.	Max Loss POD6 1990 (kt)	Max Loss POD6 1990 (%)	Max Loss POD6 2010 (kt)	Max Loss POD6 2010 (%)	Trend Loss POD6 (kt/yr)	Trend signif.
AL	361,6	12802,0	8107,9	3,9	4,2	79,0	21,9	50,9	14,1	-1,5	0,00	54,9	15,2	58,9	16,3	0,1	0,65
AT	2082,2	14643,0	9192,0	2,7	2,9	470,1	22,6	260,8	12,5	-10,8	0,00	282,0	13,5	325,4	15,6	2,6	0,17
BA	599,3	11074,0	6426,9	4,0	4,1	115,4	19,3	70,3	11,7	-2,2	0,00	76,0	12,7	81,2	13,6	0,2	0,88
BE	2190,1	10240,3	4582,0	5,5	4,6	367,9	16,8	172,8	7,9	-9,8	0,00	471,0	21,5	389,7	17,8	-3,1	0,19
BG	4520,8	12104,3	7370,1	1,6	2,1	933,7	20,7	576,2	12,7	-16,7	0,00	180,4	4,0	232,8	5,1	4,3	0,16
CH	715,6	17956,5	9045,0	2,5	2,0	198,2	27,7	88,3	12,3	-5,7	0,00	137,7	19,2	102,9	14,4	-1,7	0,12
CY	26,3	14433,6	11628,7	2,2	1,1	6,8	25,9	5,5	21,0	-0,1	0,00	2,2	8,2	1,0	3,7	0,0	0,06
CZ	5093,0	11876,8	6519,4	4,2	4,2	1029,6	20,2	576,2	11,3	-23,8	0,00	762,6	15,0	806,5	15,8	1,9	0,83
DE	22837,9	11537,6	5698,3	5,0	4,2	4460,5	19,5	2223,0	9,7	-113,1	0,00	4459,0	19,5	3733,3	16,3	-35,8	0,14
DK	4743,8	5789,3	3959,8	2,4	2,6	541,5	11,4	360,0	7,6	-10,3	0,01	536,8	11,3	536,6	11,3	2,0	0,88
EE	151,1	3049,8	2235,1	1,3	2,1	8,2	5,5	6,4	4,2	-0,1	0,09	8,1	5,4	12,1	8,0	0,2	0,19
ES	5898,0	12547,6	9952,9	2,7	3,0	1210,1	20,5	949,0	16,1	-13,8	0,24	547,3	9,3	633,9	10,7	6,1	0,45
FI	427,5	1785,7	1161,6	0,3	0,7	22,3	5,2	15,2	3,6	-0,4	0,01	11,5	2,7	21,7	5,1	0,4	0,38
FR	36195,6	11453,0	5752,8	4,7	4,0	6690,4	18,5	3164,7	8,7	-175,2	0,00	6899,6	19,1	5810,0	16,1	-65,0	0,07
GR	2590,5	16789,3	12410,2	2,8	2,6	601,9	23,2	373,0	14,4	-10,8	0,00	260,8	10,1	331,8	12,8	4,5	0,35
HR	1274,6	14137,5	8388,3	3,7	3,7	279,0	21,9	169,4	13,3	-5,6	0,00	153,0	12,0	157,9	12,4	0,2	0,98
HU	4874,0	12079,6	7340,1	2,5	2,8	994,9	20,4	624,6	12,8	-19,3	0,01	410,5	8,4	469,1	9,6	4,4	0,74
IE	712,6	3884,8	2042,9	1,3	0,6	50,9	7,1	28,2	4,0	-1,2	0,01	42,1	5,9	21,0	3,0	-1,0	0,22
IS	0,0	651,0	804,5	0,0	0,0	0,0	0,0	0,0	0,0	0,0	1,00	0,0	0,0	0,0	0,0	1,00	
IT	7271,5	22169,5	14144,4	3,9	4,0	2539,8	34,9	1597,4	22,0	-49,1	0,00	1161,3	16,0	1269,1	17,5	8,4	0,53
LI	14,6	17948,3	9090,2	0,3	0,6	4,3	29,4	2,1	14,1	-0,1	0,00	0,5	3,2	0,7	4,7	0,0	0,22
LT	1262,0	3627,9	2285,7	3,4	2,8	85,1	6,7	57,4	4,6	-1,4	0,02	163,1	12,9	130,4	10,3	-2,0	0,22
LU	177,3	12371,2	4312,2	4,6	3,4	37,1	20,9	12,4	7,0	-1,1	0,00	29,9	16,9	20,2	11,4	-0,6	0,09
LV	570,4	3096,8	2114,2	2,5	2,5	32,3	5,7	22,9	4,0	-0,5	0,10	55,5	9,7	51,3	9,0	-0,1	0,88
ME	93,3	10476,8	6353,9	3,6	3,8	15,8	16,9	10,2	10,9	-0,3	0,00	12,6	13,5	13,1	14,1	0,0	0,98
MK	603,5	11320,7	7311,1	1,2	2,4	122,5	20,3	76,1	12,6	-2,2	0,00	18,2	3,0	47,0	7,8	1,8	0,03
MT	9,4	24620,5	16390,8	0,7	0,8	3,8	40,4	2,6	27,7	-0,1	0,00	0,2	2,2	0,2	2,6	0,0	0,61
NL	1685,8	8543,3	4548,5	4,8	3,9	255,3	15,1	141,0	8,4	-5,7	0,01	358,3	21,3	290,6	17,2	-3,4	0,12
NO	269,2	1943,6	1368,7	0,1	0,2	20,7	7,7	13,2	4,9	-0,4	0,03	11,9	4,4	11,1	4,1	0,0	0,93
PL	9860,0	8146,2	4567,7	4,3	3,7	1448,7	14,7	844,7	8,6	-31,6	0,00	1639,3	16,6	1428,0	14,5	-11,0	0,32
PT	413,4	11126,0	8561,1	2,9	3,0	78,6	19,0	62,6	15,1	-0,5	0,49	31,8	7,7	35,7	8,6	0,4	0,57
RO	6981,0	9241,9	5677,1	1,9	1,8	1253,5	18,0	786,7	11,3	-23,0	0,01	271,1	3,9	278,4	4,0	3,0	0,53
RS	2805,9	11431,2	7078,0	1,6	2,8	584,4	20,8	366,4	13,1	-13,6	0,00	112,8	4,0	240,8	8,6	5,8	0,14
SE	2164,0	2721,8	1715,7	0,8	0,9	202,3	9,3	127,6	5,9	-4,1	0,01	213,9	9,9	224,3	10,4	-0,2	0,98
SI	344,5	16392,4	8969,6	5,2	4,8	86,0	25,0	50,3	14,6	-1,8	0,00	51,5	14,9	52,1	15,1	-0,2	0,79
SK	1867,4	10873,4	6338,1	3,1	3,7	353,9	19,0	213,3	11,4	-7,4	0,00	179,6	9,6	238,0	12,7	3,9	0,45
UK	14393,5	4492,7	2469,3	1,9	1,1	1432,2	10,0	813,0	5,6	-39,1	0,00	2157,8	15,0	1367,2	9,5	-39,8	0,03
EEA38	146081,2	10749,8	6498,2	2,8	2,8	26616,7	18,2	14914,4	10,2	-591,2	0,00	21764,4	14,9	19424,2	13,3	-109,7	0,11

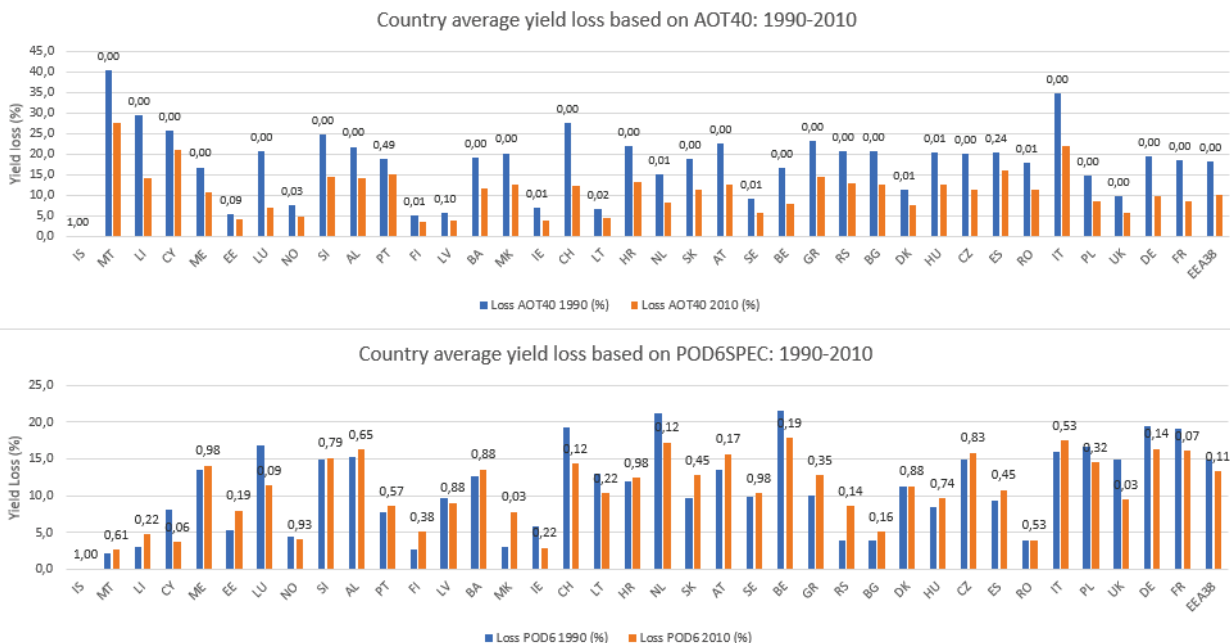


Figure 18: Percentage wheat crop yield losses representative of 1990 and 2010 in European countries (sorted by increasing wheat production) when using either the AOT40 or POD<sub>6</sub>SPEC indicator. Instead of providing the actual value for 1990 or 2010, we provide an estimate based on the linear fit of the trend for 1990 or 2010 to minimize the impact of interannual variability. For each country, the significance of the trend between 1990 and 2010 is provided (numbers above the histograms) and considered significant when lower than 0.05.

## 4 Conclusion/Discussion

The most cited detrimental impacts of air pollution are generally concerning human health (notably due to exposure to fine particulate matter) or ecosystem (as a result to acidification or eutrophication). Detrimental impacts of ozone air pollution on ecosystems is also noteworthy. In the 2008 European Directive on Ambient Air Quality (EC, 2008), such impacts are estimated using an exposure metric: the accumulated ozone above a threshold of 40 ppb (AOT40), for which both a target value and long-term objectives are set. The application of this metric in risk assessments has been criticized in recent decades as it only takes into account atmospheric ozone concentrations and ignores environmental factors such as temperature, soil moisture, water vapor or even the plant phenology, that affect ozone uptake by vegetation. Hence, a biologically more relevant dose indicator was developed, which is based on the ozone stomatal uptake by the plants: the Photosynthetic Ozone Dose above a flux-threshold Y (POD<sub>Y</sub>).

In the current report, we compared both metrics, computed either from in-situ observations of ozone concentrations or chemistry-transport models. AOT40 is based exclusively on hourly ozone concentrations, it can therefore be readily computed from either observations or model outputs. POD<sub>Y</sub> is of course also a function of atmospheric ozone concentrations, but it also accounts for other environmental factors (temperature, soil moisture, incoming solar radiation, water vapour) and the phenology of the plant, affecting ozone uptake by the plant. A new computer program was developed in order to derive the POD<sub>Y</sub> levels corresponding to either observation or model results in a consistent manner. The methodology follows the recommendations from the Working Group on Effects of the Geneva Convention on the Long Range Transboundary Air Pollution (CLRTAP, 2017). That methodology is however in constant evolution, and possible improvements have been identified for instance in differentiating irrigated and non-irrigated crops (as it has a strong impact on soil moisture while no distinction was made in the present study). The POD<sub>Y</sub> metric we used here is specific for wheat (POD<sub>6</sub>SPEC) and more specifically bread wheat (*Triticum aestivum*). Information on the potential risk of ozone effects on yield quality as well as on other economically important crops, such as horticultural

crops, is available and more indicators will be made available in the future. Last, the present approach is taking into account only direct effects of ozone on yield but interactions with nitrogen fertilization, drought and diseases have been also described but cannot be currently quantified.

The relevance of including model results relies mainly in their exhaustive geographical coverage, whereas the representativeness is limited for in-situ surface observations. Such an exhaustive coverage allows using the exposure or dose estimate to discuss the actual negative impact of ozone pollution on wheat yield. In addition, the model results used here cover a long period of time (1990-2010), for which only scatter measurements are available in some parts of Europe, especially in the early 1990s.

Chemistry-transport models may however suffer from biases, especially when raw model outputs are used without any data assimilation or data fusion (that would merge model results and actual observations). This shortcoming is minimized here by relying on an ensemble of models (the Eurodelta-Trend multi-model ensemble) rather than a unique source.

The comparison between the Eurodelta-Trends ensemble of models and observations in terms of trends of ozone dose and exposure shows that the performances are similar for four out of the five models involved. One model exhibits higher ozone concentrations, but that bias has a limited impact on the estimate of POD<sub>6</sub>SPEC. The models manage to capture well the trend in POD<sub>6</sub>SPEC, but overestimate the magnitude of decrease of AOT40, especially for the 1990s. Since we relied here on an ensemble of chemistry-transport models, this bias is attributed to the common forcing emission trends used by all models.

The wheat yield loss reported here due to ozone pollution is remarkably similar to earlier published losses with an estimate for the year 2000 of 13.9%, which is similar to the 14% yield loss reported by (Pleijel et al., 2014) and the 13% reported by (Mills and Harmens, 2011).

The reported long-term trends of the impact of ozone air pollution on crop yield across Europe are notably different when using the AOT40 or POD<sub>6</sub>SPEC metric. For AOT40 we found that the negative impact on crop yield decreased significantly from 18.2% to 10.2% between 1990 and 2010. For POD<sub>6</sub>SPEC, the trend is non-significant and changes from 14.9 to 13.3% over the same time period. The validation of models against observations still includes substantial uncertainties, especially because the network coverage is scarce in the 1990s. For the 2000-2010 decade (when the confidence on model performances is higher), we find again a lack of significant trend according to POD<sub>6</sub>SPEC (when ozone reduces wheat yield by 13.3% in 2010), while AOT40 points towards an improvement with a decrease of wheat yield loss from 13.5% to 10.2% between 2000 and 2010. The reasons for the discrepancy between the AOT40 and POD<sub>6</sub>SPEC trends include: (i) influence of changing ozone concentration profiles (decreases in peak ozone concentration, increases or no trends in average ozone concentration), and (ii) influence of meteorological conditions including soil moisture trends (yielding a higher ozone uptake for a given ozone exposure).

Even if uncertainties remain with such an assessment based on numerical models, only such tools allow coverage for the whole of Europe over a long-time period to investigate the evolution of ozone pollution impacts on wheat yield. The most robust findings of this study are that: (i) the impact of ozone on wheat yield varied between 10 to 20% in Europe over the 1990-2010 time period depending on the metric applied, (ii) the trends are very sensitive to the selected metric with a significant decline in detrimental ozone impacts found when using AOT40, whereas the flux-based dose formulation indicated no improvement.

## References

- Amann, M., Borken-Kleefeld, J., Cofala, J., Heyes, C., Klimont, Z., Rafaj, P., Purohit, P., Schoepp, W., and Winiwarter, W.: Future emissions of air pollutants in Europe - Current legislation baseline and the scope for further reductions., IIASA, Laxenburg, Austria, 2012.
- Andersson, C., Alpfjord, H., Robertson, L., Karlsson, P. E., and Engardt, M.: Reanalysis of and attribution to near-surface ozone concentrations in Sweden during 1990–2013, *Atmos. Chem. Phys.*, 17, 13869–13890, 10.5194/acp-17-13869-2017, 2017.
- CLRTAP: Chapter III: "Mapping Critical levels for Vegetation", UNECE Convention on Long Range Transboundary Air Pollution, Geneva, 2017.
- Colette, A., Aas, W., Banin, L., Braban, C. F., Ferm, M., González Ortiz, A., Ilyin, I., Mar, K., Pandolfi, M., Putaud, J.-P., Shatalov, V., Solberg, S., Spindler, G., Tarasova, O., Vana, M., Adani, M., Almodovar, P., Berton, E., Bessagnet, B., Bohlin-Nizzetto, P., Boruvkova, J., Breivik, K., Briganti, G., Cappelletti, A., Cuvelier, K., Derwent, R., D'Isidoro, M., Fagerli, H., Funk, C., Garcia Vivanco, M., Haeuber, R., Hueglin, C., Jenkins, S., Kerr, J., de Leeuw, F., Lynch, J., Manders, A., Mircea, M., Pay, M. T., Pritula, D., Querol, X., Raffort, V., Reiss, I., Roustan, Y., Sauvage, S., Scavo, K., Simpson, D., Smith, R. I., Tang, Y. S., Theobald, M., Tørseth, K., Tsyro, S., van Pul, A., Vidic, S., Wallasch, M., and Wind, P.: Air pollution trends in the EMEP region between 1990 and 2012, NILU, Oslo, 2016.
- Colette, A., Andersson, C., Manders, A., Mar, K., Mircea, M., Pay, M. T., Raffort, V., Tsyro, S., Cuvelier, C., Adani, M., Bessagnet, B., Bergström, R., Briganti, G., Butler, T., Cappelletti, A., Couvidat, F., D'Isidoro, M., Doumbia, T., Fagerli, H., Granier, C., Heyes, C., Klimont, Z., Ojha, N., Otero, N., Schaap, M., Sindelarova, K., Stegehuis, A. I., Roustan, Y., Vautard, R., van Meijgaard, E., Vivanco, M. G., and Wind, P.: EURODELTA-Trends, a multi-model experiment of air quality hindcast in Europe over 1990–2010, *Geosci. Model Dev.*, 10, 3255–3276, 10.5194/gmd-10-3255-2017, 2017a.
- Colette, A., Solberg, S., Beauchamp, M., Bessagnet, B., Malherbe, L., and Guerreiro, C.: Long term air quality trends in Europe: Contribution of meteorological variability, natural factors and emissions, ETC/ACM, Bilthoven, 2017b.
- EC: Directive 2008/50/EC of the European Parliament and of the Council of 21 May 2008 on ambient air quality and cleaner air for Europe, European Commission, Brussels, 2008.
- EEA: Air quality in Europe — 2012 report, European Environmental Agency, Copenhagen12/2012, 2012.
- EEA: Air quality in Europe — 2013 report, European Environment Agency, Copenhagen, 112, 2013.
- EEA: Air Quality in Europe - 2018 Report, Copenhagen, 2018.
- Emberson, L., Ashmore, M., Cambridge, H., Simpson, D., and Tuovinen, J.-P.: Modelling stomatal ozone flux across Europe, *Environmental Pollution*, 109, 403–413, 2000a.
- Emberson, L. D., Ashmore, M. R., Simpson, D., Tuovinen, J.-P., and Cambridge, H. M.: Modelling stomatal ozone flux across Europe, *Water, Air and Soil Pollution*, 109, 403–413, 2000b.
- Grünhage, L., Pleijel, H., Mills, G., Bender, J., Danielsson, H., Lehmann, Y., Castell, J.-F., and Bethenod, O.: Updated stomatal flux and flux-effect models for wheat for quantifying effects of ozone on grain yield, grain mass and protein yield, *Environmental Pollution*, 165, 147–157, <https://doi.org/10.1016/j.envpol.2012.02.026>, 2012.
- Hanel, M., Rakovec, O., Markonis, Y., Máca, P., Samaniego, L., Kyselý, J., and Kumar, R.: Revisiting the recent European droughts from a long-term perspective, *Scientific Reports*, 8, 9499, 10.1038/s41598-018-27464-4, 2018.
- Holobaca, I., Sorocovschi, V., and Dubreuil, V.: Suivi par télédétection de la sécheresse de l'année 2000 dans la dépression de la Transylvanie, *Climatologie*, 15, 87–94, 2003.
- Horálek, J., de Smet, P., Corbet, L., Kurfürst, P., and de Leeuw, F.: European air quality maps of PM and ozone for 2010 and their uncertainty, Bilthoven, 2012.
- Jacob, D., Petersen, J., Eggert, B., Alias, A., Christensen, O., Bouwer, L., Braun, A., Colette, A., Déqué, M., Georgievski, G., Georgopoulou, E., Gobiet, A., Menut, L., Nikulin, G., Haensler, A., Hempelmann, N., Jones, C., Keuler, K., Kovats, S., Kraner, N., Kotlarski, S., Kriegsmann, A., Martin, E., Meijgaard, E., Moseley, C., Pfeifer, S., Preuschmann, S., Radermacher, C., Radtke, K., Rechid, D., Rounsevell, M., Samuelsson, P., Somot, S., Soussana, J.-F., Teichmann, C., Valentini, R., Vautard, R., Weber, B.,

- and Yiou, P.: EURO-CORDEX: new high-resolution climate change projections for European impact research, *Regional Environmental Change*, 1-16, 2013.
- Jarvis, P.: The interpretation of the variations in leaf water potential and stomatal conductance found in canopies in the field, *Phil. Trans. R. Soc. Lond. B*, 273, 593-610, 1976.
- Karlsson, P. E., Klingberg, J., Engardt, M., Andersson, C., Langner, J., Karlsson, G. P., and Pleijel, H.: Past, present and future concentrations of ground-level ozone and potential impacts on ecosystems and human health in northern Europe, *Science of the Total Environment*, 576, 22-35, 2017.
- Klimont, Z., Kupiainen, K., Heyes, C., Purohit, P., Cofala, J., Rafaj, P., Borken-Kleefeld, J., and Schöpp, W.: Global anthropogenic emissions of particulate matter including black carbon, *Atmos. Chem. Phys.*, 17, 8681-8723, 10.5194/acp-17-8681-2017, 2017.
- Lefohn, A. S., Malley, C. S., Simon, H., Wells, B., Xu, X., Zhang, L., and Wang, T.: Responses of human health and vegetation exposure metrics to changes in ozone concentration distributions in the European Union, United States, and China, *Atmospheric Environment*, 152, 123-145, <http://dx.doi.org/10.1016/j.atmosenv.2016.12.025>, 2017.
- McNaughton, K., and Van den Hurk, B.: A 'Lagrangian' revision of the resistors in the two-layer model for calculating the energy budget of a plant canopy, *Boundary-Layer Meteorology*, 74, 261-288, 1995.
- Mills, G., Buse, A., Gimeno, B., Bermejo, V., Holland, M., Emberson, L., and Pleijel, H.: A synthesis of AOT40-based response functions and critical levels of ozone for agricultural and horticultural crops, *Atmospheric Environment*, 41, 2630-2643, <https://doi.org/10.1016/j.atmosenv.2006.11.016>, 2007.
- Mills, G., and Harmens, H.: Ozone Pollution: A hidden threat to food security, Centre for Ecology and Hydrology, Gwynedd, 2011.
- Mills, G., Pleijel, H., Malley, C. S., Sinha, B., Cooper, O. R., Schultz, M. G., Neufeld, H. S., Simpson, D., Sharps, K., and Feng, Z.: Tropospheric Ozone Assessment Report: Present-day tropospheric ozone distribution and trends relevant to vegetation, *Elementa: Science of the Anthropocene*, 6, 2018.
- Pleijel, H., Danielsson, H., Simpson, D., and Mills, G.: Have ozone effects on carbon sequestration been overestimated? A new biomass response function for wheat, *Biogeosciences*, 11, 4521-4528, 2014.
- Simpson, D., Ashmore, M., Emberson, L., and Tuovinen, J.-P.: A comparison of two different approaches for mapping potential ozone damage to vegetation. A model study, *Environmental Pollution*, 146, 715-725, 2007.
- Simpson, D., Benedictow, A., Berge, H., Bergstrom, R., Emberson, L. D., Fagerli, H., Flechard, C. R., Hayman, G. D., Gauss, M., Jonson, J. E., Jenkin, M. E., Nyiri, A., Richter, C., Semeena, V. S., Tsyró, S., Tuovinen, J. P., Valdebenito, A., and Wind, P.: The EMEP MSC-W chemical transport model - technical description, *Atmos. Chem. Phys.*, 12, 7825-7865, 2012.
- Simpson, D., Arneth, A., Mills, G., Solberg, S., and Uddling, J.: Ozone - the persistent menace: interactions with the N cycle and climate change, *Current Opinion in Environmental Sustainability*, 9-10, 9-19, 2014.
- Skamarock, W. C., Klemp, J. B., Dudhia, J., Gill, D. O., Barker, D. M., Duda, M. G., Huang, X. Y., Wang, W., and Powers, J. G.: A Description of the Advanced Research WRF Version 3, NCAR, 2008.
- Spinoni, J., Naumann, G., and Vogt, J. V.: Pan-European seasonal trends and recent changes of drought frequency and severity, *Global and Planetary Change*, 148, 113-130, <https://doi.org/10.1016/j.gloplacha.2016.11.013>, 2017.
- Stegehuis, A. I., Vautard, R., Ciais, P., Teuling, A. J., Miralles, D. G., and Wild, M.: An observation-constrained multi-physics WRF ensemble for simulating European mega heat waves, *Geosci. Model Dev.*, 8, 2285-2298, 10.5194/gmd-8-2285-2015, 2015.
- Tuovinen, J.-P., and Simpson, D.: An aerodynamic correction for the European ozone risk assessment methodology, *Atmospheric Environment*, 42, 8371-8381, <https://doi.org/10.1016/j.atmosenv.2008.08.008>, 2008.

## Annex 1 – Ozone in Europe in the absence of anthropogenic emissions

A sensitivity experiment was performed to investigate wheat yield losses in the absence of either anthropogenic or biogenic European precursor emissions of ozone. Since those experiments were not planned in the Eurodelta-Trends setup, the tests were only performed with the Chimere CTM. The corresponding maps for ozone annual mean, summertime ozone peaks, AOT40 and POD6SPEC are provided in Figure 19 to 22.

Ozone annual mean concentrations decrease when either anthropogenic or biogenic emissions are removed (Figure 19). The reduction of ozone annual mean when biogenic emissions are removed is quite uniform across Europe and below 20%. When removing anthropogenic emission, the reduction can reach 30% over the Mediterranean, but ozone annual mean can also increase 30 to 40% in NO<sub>x</sub>-saturated areas (large cities in North and Western Europe) because of the titration effect of NO<sub>x</sub>.

For the summertime (June, July, August) average of daily peaks (Figure 20), the reduction when removing anthropogenic emission can reach 30-40% over Continental Europe, or even larger than 50% over the Mediterranean Sea. There are still marginal increases limited to the English Channel. Biogenic emissions have also an impact, about half as large as that of Anthropogenic emissions.

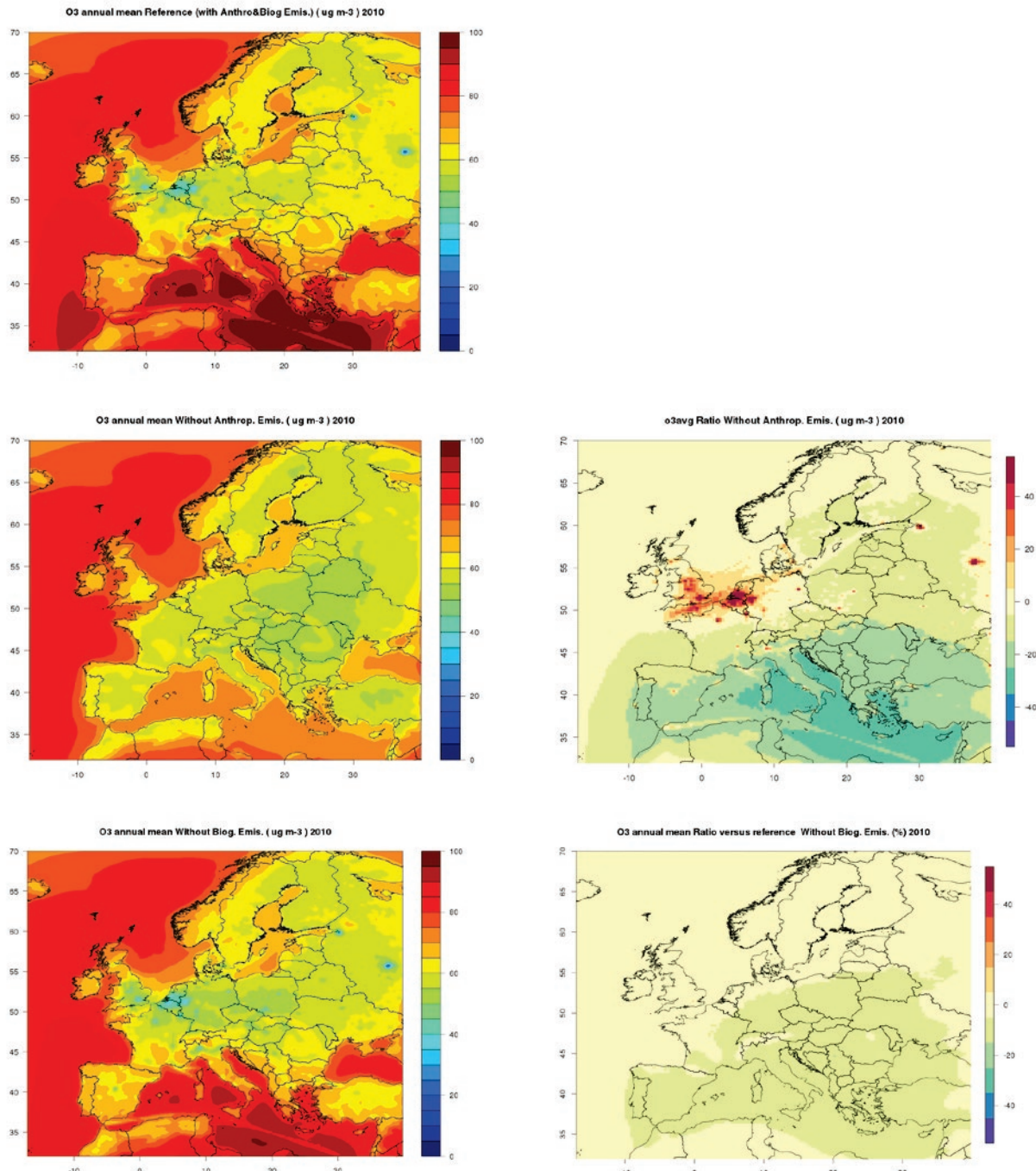


Figure 19: Left: map of annual mean ozone ( $\mu\text{g}/\text{m}^3$ ) in a CHIMERE simulation for 2010 with all emissions included (top), with European anthropogenic emissions ignored (middle) and with European biogenic emissions ignored (bottom). Right: relative differences compared to the simulation including all emissions (in %).

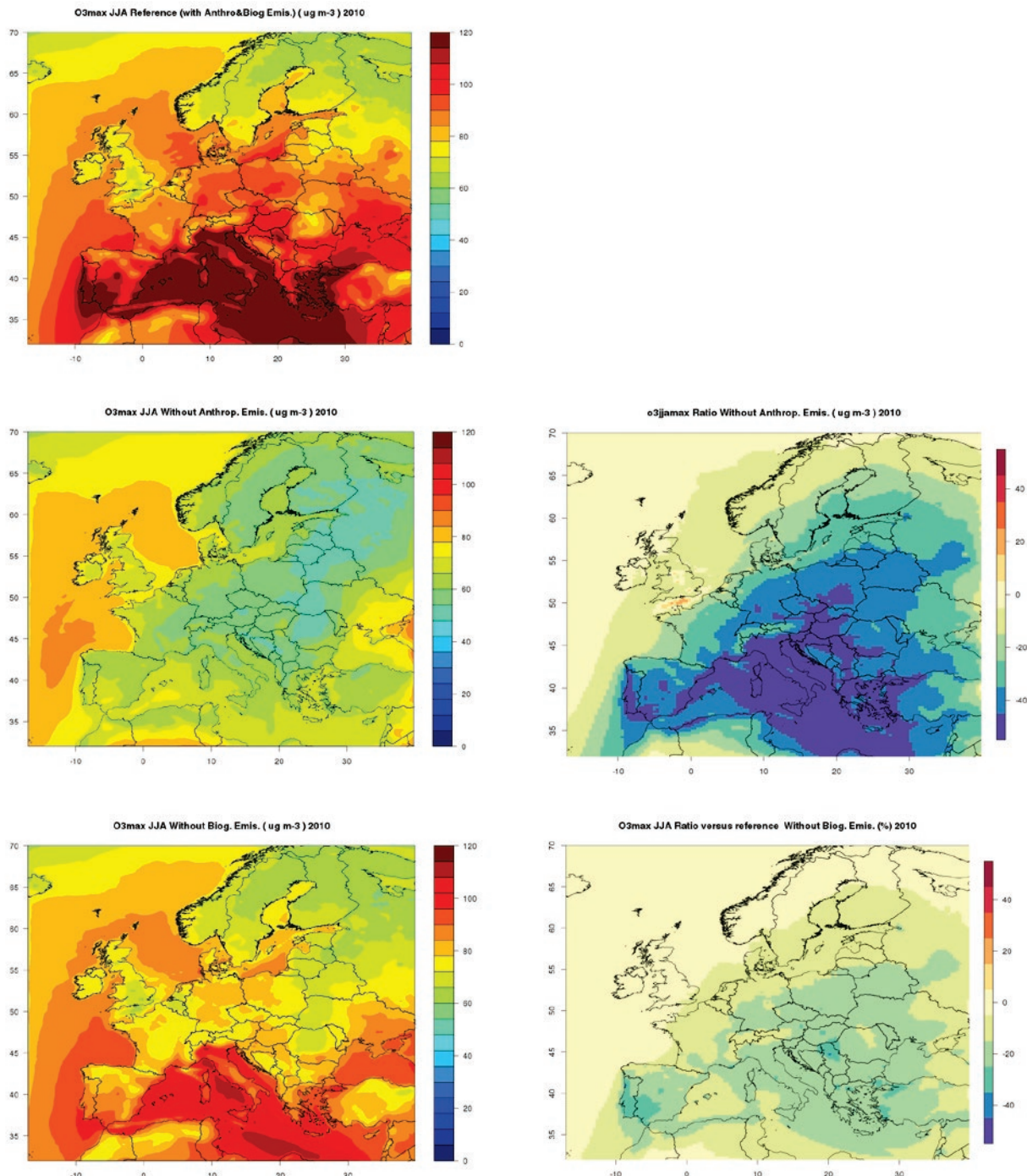


Figure 20: Same as Figure 19 for the summertime (June-July-August) average of daily maxima ( $\mu\text{g/m}^3$ )

The maps of Figure 21 and Figure 22, also present the results of these model sensitivity simulations but for the exposure and dose metrics AOT40 and POD<sub>6</sub>SPEC, respectively. They demonstrate that both metrics are efficient to capture the impact of ozone anthropogenic pollution, as the reduction when removing anthropogenic sources reaches 100%, down to very low AOT40 and POD<sub>6</sub>SPEC levels. Scattered low levels of POD<sub>6</sub>SPEC remain close to coastlines. It is likely that long-range transboundary ozone pollution is responsible for these limited area of exposure since only European sources of anthropogenic precursor emissions were shut down in that simulation that still accounts for global chemical boundary conditions.

When anthropogenic emissions are ignored, the corresponding impact on wheat yield totals only 1.5% of the European production which, considering the uncertainties of such an assessment, is close enough to

zero to conclude that the POD<sub>6</sub>SPEC metric implemented here is selective for the purpose of our assessment, otherwise an offset should have been considered to isolate the impact of anthropogenic ozone alone.

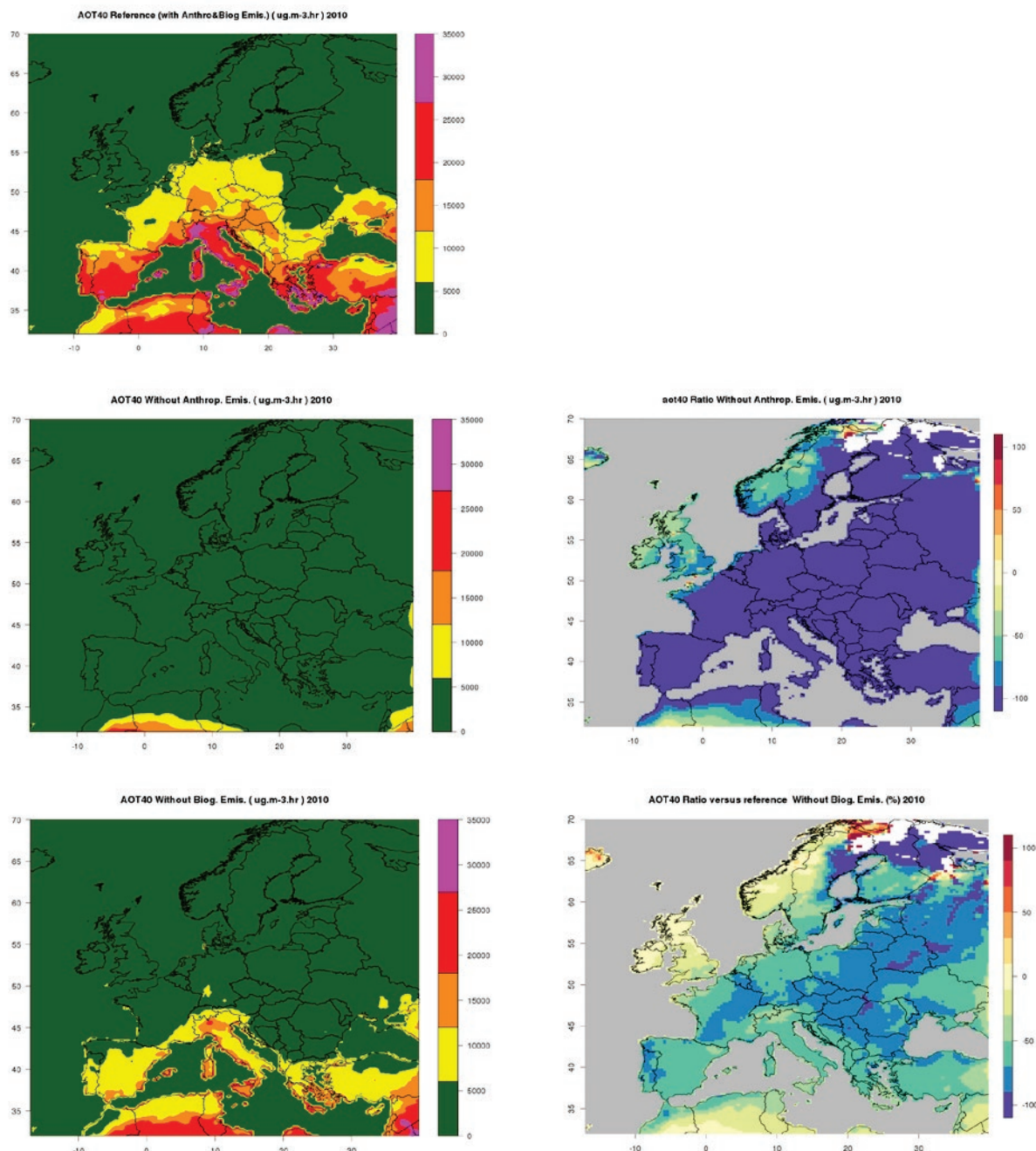


Figure 21: Same as Figure 19 for AOT40 ( $\mu\text{g}/\text{m}^3.\text{hr}$ )

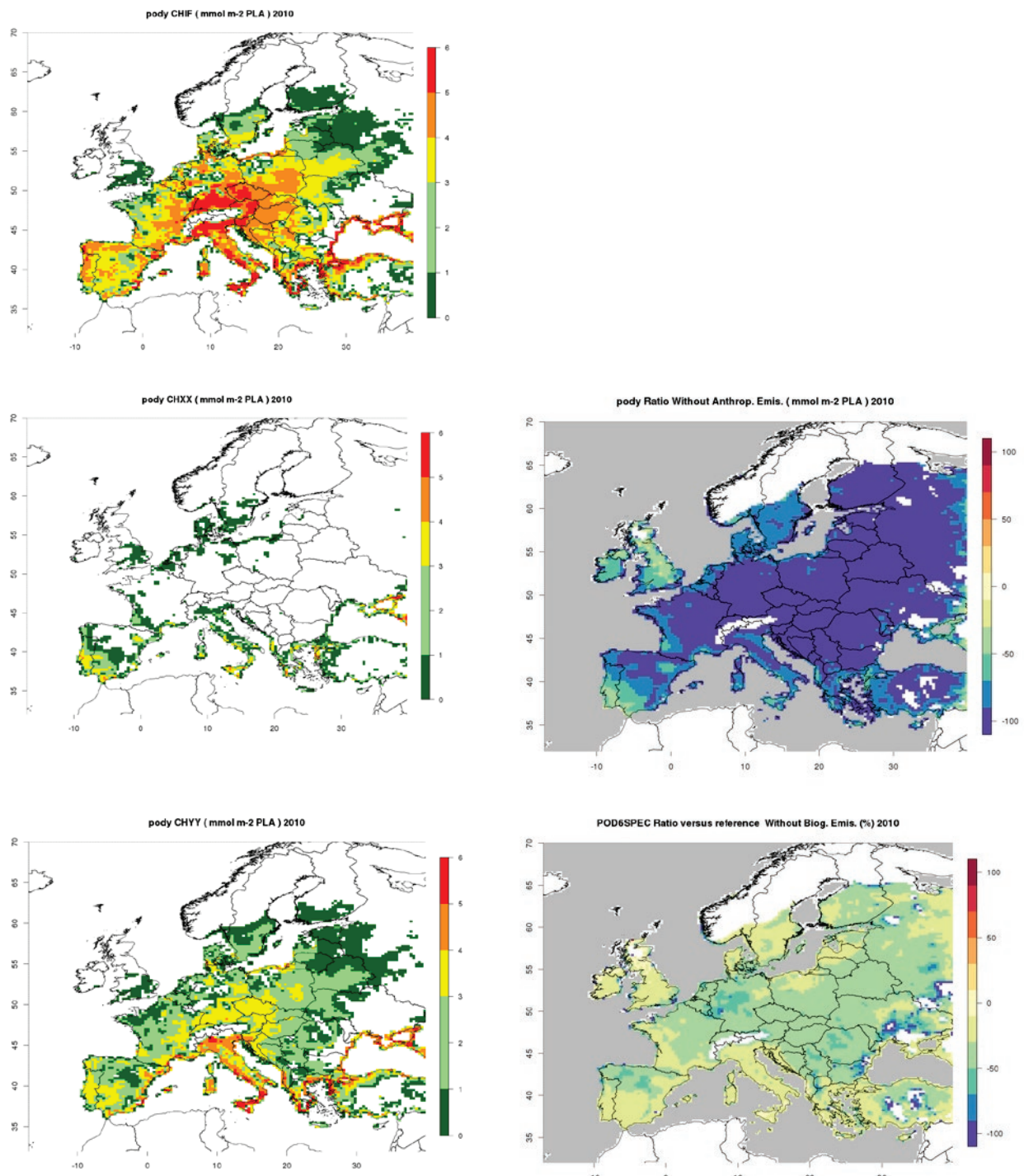


Figure 22: Same as Figure 19 for POD<sub>6</sub>SPEC (mmol.m<sup>-2</sup> PLA)

## Annex 2 – Exposure and losses by country

Table 3: Same as Table 2 for the 2000-2010 period

Country	Wheat Production (kt)	AOT40 2000		AOT40 2010		POD6 2000		POD6 2010		Max Loss AOT40 2000 (kt)	Max Loss AOT40 2000 (%)	Max Loss AOT40 2010 (kt)	Max Loss AOT40 2010 (%)	Trend Loss AOT40 (kt/yr)	Trend Signif.	Max Loss POD6 2000 (kt)	Max Loss POD6 2000 (%)	Max Loss POD6 2010 (kt)	Max Loss POD6 2010 (%)	Trend Loss POD6 (kt/yr)	Trend signif.
		AOT40	2000	AOT40	2010	POD6	2000	POD6	2010												
AL	361,6	9732,0	8107,9	4,0	4,2	59,6	16,5	50,9	14,1	-1,6	0,09	57,4	15,9	58,9	16,3	0,1	0,88				
AT	2082,2	11722,6	9192,0	2,8	2,9	373,6	17,9	260,8	12,5	-13,5	0,01	306,4	14,7	325,4	15,6	5,3	0,28				
BA	599,3	7805,9	6426,9	4,1	4,1	85,1	14,2	70,3	11,7	-2,6	0,12	81,8	13,6	81,2	13,6	1,2	0,64				
BE	2190,1	7442,0	4582,0	5,3	4,6	273,2	12,5	172,8	7,9	-6,9	0,16	455,5	20,8	389,7	17,8	-2,0	0,64				
BG	4520,8	9171,0	7370,1	1,2	2,1	708,1	15,7	576,2	12,7	-29,0	0,16	101,1	2,2	232,8	5,1	11,3	0,09				
CH	715,6	13753,7	9045,0	1,9	2,0	126,7	17,7	88,3	12,3	-5,1	0,01	103,0	14,4	102,9	14,4	-0,6	0,64				
CY	26,3	12893,4	11628,7	2,4	1,1	6,2	23,6	5,5	21,0	-0,1	0,06	2,3	8,9	1,0	3,7	0,0	0,44				
CZ	5093,0	9806,8	6519,4	4,1	4,2	838,1	16,5	576,2	11,3	-30,3	0,06	761,8	15,0	806,5	15,8	16,6	0,64				
DE	22837,9	8267,2	5698,3	4,6	4,2	3239,6	14,2	2223,0	9,7	-98,8	0,09	4079,4	17,9	3733,3	16,3	-39,3	0,64				
DK	4743,8	5390,1	3959,8	2,4	2,6	451,1	9,5	360,0	7,6	-15,0	0,06	506,9	10,7	536,6	11,3	-3,0	0,88				
EE	151,1	3106,8	2235,1	1,4	2,1	8,4	5,6	6,4	4,2	-0,3	0,16	9,2	6,1	12,1	8,0	0,1	0,76				
ES	5898,0	10410,7	9952,9	2,5	3,0	1002,2	17,0	949,0	16,1	-46,6	0,16	482,6	8,2	633,9	10,7	-1,6	1,00				
FI	427,5	1701,2	1161,6	0,4	0,7	19,7	4,6	15,2	3,6	-0,7	0,09	11,9	2,8	21,7	5,1	-0,1	1,00				
FR	36195,6	7398,5	5752,8	4,6	4,0	3890,8	10,7	3164,7	8,7	-146,7	0,16	6863,7	19,0	5810,0	16,1	-107,4	0,28				
GR	2590,5	14554,6	12410,2	2,9	2,6	475,4	18,4	373,0	14,4	-14,0	0,12	180,5	7,0	331,8	12,8	6,9	0,53				
HR	1274,6	10647,1	8388,3	4,6	3,7	204,9	16,1	169,4	13,3	-7,1	0,12	192,9	15,1	157,9	12,4	1,5	0,88				
HU	4874,0	9871,3	7340,1	2,1	2,8	822,0	16,9	624,6	12,8	-35,4	0,16	327,9	6,7	469,1	9,6	16,2	0,44				
IE	712,6	3407,3	2042,9	0,6	0,6	46,3	6,5	28,2	4,0	-1,8	0,09	16,0	2,2	21,0	3,0	-0,6	0,64				
IS	0,0	739,9	804,5	0,0	0,0	0,0	NaN	0,0	NaN	0,0	1,00	0,0	NaN	0,0	NaN	0,0	1,00				
IT	7271,5	17331,9	14144,4	4,6	4,0	1979,3	27,2	1597,4	22,0	-60,6	0,02	1481,4	20,4	1269,1	17,5	-31,2	0,53				
LI	14,6	13595,0	9090,2	0,3	0,6	3,0	20,6	2,1	14,1	-0,1	0,01	0,4	2,8	0,7	4,7	0,0	0,64				
LT	1262,0	3488,2	2285,7	2,4	2,8	82,3	6,5	57,4	4,6	-3,2	0,09	119,3	9,5	130,4	10,3	-1,8	0,76				
LU	177,3	7098,2	4312,2	3,9	3,4	20,6	11,6	12,4	7,0	-0,7	0,09	24,5	13,8	20,2	11,4	-0,4	0,76				
LV	570,4	3027,4	2114,2	2,0	2,5	31,3	5,5	22,9	4,0	-1,1	0,21	43,2	7,6	51,3	9,0	-0,3	1,00				
ME	93,3	7792,3	6353,9	3,2	3,8	11,7	12,6	10,2	10,9	-0,3	0,06	10,2	10,9	13,1	14,1	-0,1	0,53				
MK	603,5	8547,6	7311,1	0,6	2,4	93,0	15,4	76,1	12,6	-2,7	0,09	5,1	0,8	47,0	7,8	2,8	0,28				
MT	9,4	17206,7	16390,8	1,5	0,8	2,7	28,8	2,6	27,7	-0,1	0,16	0,5	5,4	0,2	2,6	0,0	0,64				
NL	1685,8	7376,9	4548,5	5,0	3,9	217,8	12,9	141,0	8,4	-6,3	0,21	362,5	21,5	290,6	17,2	-6,6	0,28				
NO	269,2	2258,6	1368,7	0,1	0,2	20,5	7,6	13,2	4,9	-0,8	0,21	5,7	2,1	11,1	4,1	0,3	0,53				
PL	9860,0	7219,5	4567,7	4,2	3,7	1265,4	12,8	844,7	8,6	-46,0	0,09	1605,3	16,3	1428,0	14,5	-13,3	0,64				
PT	413,4	8753,7	8561,1	2,7	3,0	60,5	14,6	62,6	15,1	-2,9	0,16	35,7	8,6	35,7	8,6	-1,0	0,76				
RO	6981,0	8104,7	5677,1	0,9	1,8	1017,8	14,6	786,7	11,3	-38,7	0,16	110,8	1,6	278,4	4,0	20,8	0,03				
RS	2805,9	8221,8	7078,0	1,6	2,8	419,6	15,0	366,4	13,1	-15,7	0,16	104,0	3,7	240,8	8,6	28,5	0,12				
SE	2164,0	2701,9	1715,7	0,7	0,9	184,8	8,5	127,6	5,9	-7,2	0,09	224,8	10,4	224,3	10,4	2,2	1,00				
SI	344,5	12055,4	8969,6	5,0	4,8	66,2	19,2	50,3	14,6	-1,9	0,03	55,7	16,2	52,1	15,1	0,5	0,88				
SK	1867,4	9713,3	6338,1	2,5	3,7	323,7	17,3	213,3	11,4	-11,7	0,06	138,2	7,4	238,0	12,7	13,5	0,16				
UK	14393,5	3712,1	2469,3	1,2	1,1	1280,4	8,9	813,0	5,6	-46,1	0,12	1506,1	10,5	1367,2	9,5	-46,9	0,44				
EEA38	146081,2	8440,3	6498,2	2,6	2,8	19711,9	13,5	14914,4	10,2	-642,9	0,01	20374,0	13,9	19424,2	13,3	-49,7	0,53				

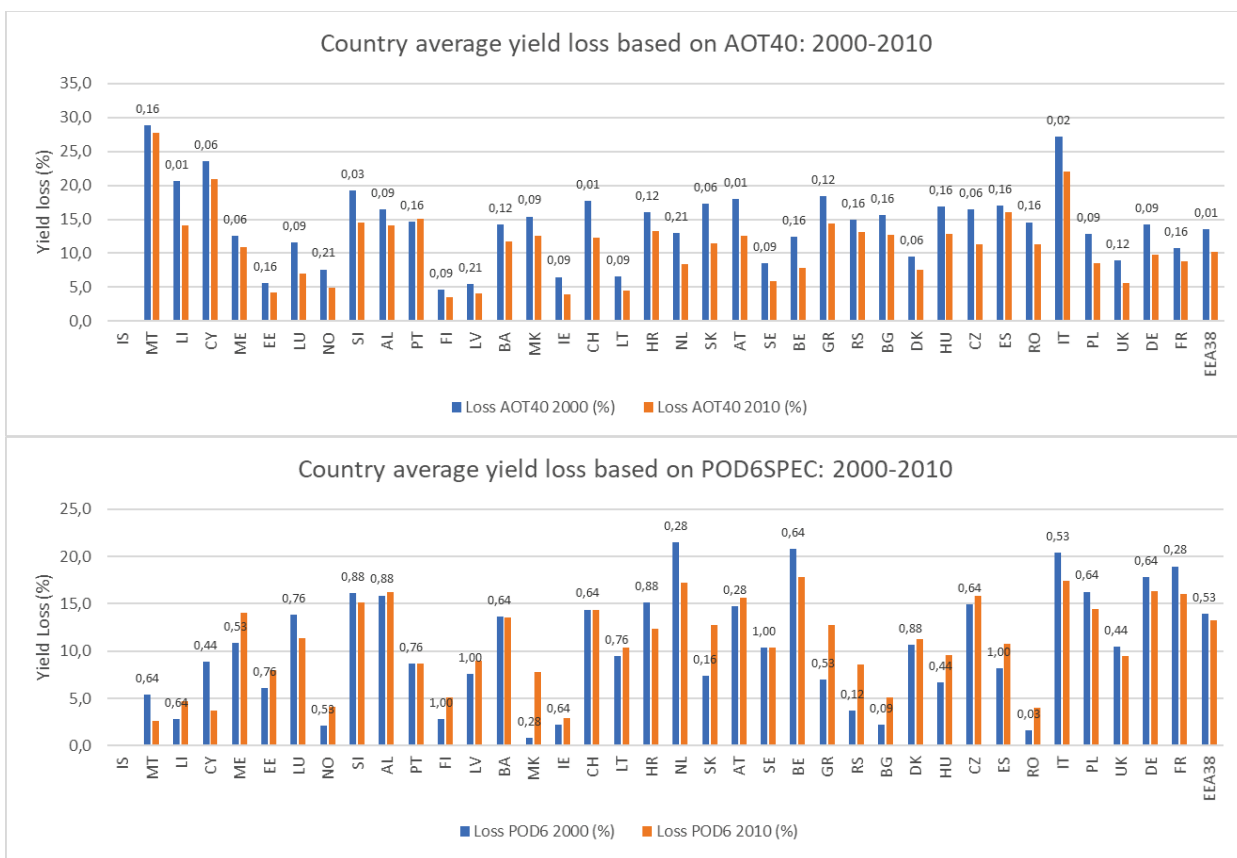


Figure 23: Same as Figure 18 for the 2000-2010 time period.



European Topic Centre on Air Pollution  
and Climate Change Mitigation  
PO Box 1  
3720 BA Bilthoven  
The Netherlands  
Tel.: +31 30 274 8562  
Fax: +31 30 274 4433  
Web: <http://acm.eionet.europa.eu>  
Email: [etcacm@rivm.nl](mailto:etcacm@rivm.nl)

The European Topic Centre on Air Pollution and Climate Change Mitigation (ETC/ACM) is a consortium of European institutes under contract of the European Environment Agency.

